*applied biosciences*

MDPI

*Article*

# Formulation by Design: Multiobjective Optimization of a Synergistic Essential Oil Blend with Bioactivities for Skin Healing Applications

**Andres Zapata Betancur [1], Freddy Forero Longas [2,*] and Adriana Pulido Diaz [3]**

[1] Pharmacy Department, University of Antioquia UdeA, Calle 67, 53-108, Medellin 050010, Colombia; andres.zapatab@udea.edu.co
[2] Food Engineering Department, University of Antioquia UdeA, Calle 67, 53-108, Medellin 050010, Colombia
[3] Agrosavia, La Selva Research Center, Rionegro 055038, Colombia; apulido@agrosavia.co
* Correspondence: freddy.forero@udea.edu.co

**Abstract**

Growing interest in natural therapies has increased the demand for essential oils; however, the complex interactions within their mixtures that dictate their final efficacy remain poorly understood. This study aimed to optimize a blend of ginger, cinnamon, tea tree, and geranium essential oils to develop an active ingredient, with synergistic multifunctional bioactivities, that was relevant to cutaneous healing. Initially, the composition and cytotoxicity for individual oils were determined; subsequently, a D-optimal mixture design was employed to evaluate three biological responses related to skin recovery: ultraviolet B radiation absorption, red blood cell lysis inhibition, and catalase enzyme activity. GC-FID analysis revealed the following major components (% *w*/*w*): cinnamon (cinnamaldehyde, 77.56%), ginger (α-zingiberene, 33.77%), geranium (citronellol, 33.6%), and tea tree (terpinen-4-ol, 38.38%). Dose–response data from essential oils tested against Detroit ATCC 551 skin fibroblasts revealed a clear cytotoxic hierarchy ($IC_{50}$ µg/mL): cinnamon (21.03) > ginger (25.3) > tea tree (41.67) > geranium (92.51). Cinnamaldehyde content was the primary contributor to photoprotective capacity, with a maximum sun protection factor (SPF) of 4.5. Inhibition against erythrocyte membrane lysis was not attributable to a single component; maximum protection (98.4%) was achieved through synergy between oxygenated monoterpenoids (geranium and tea tree), sesquiterpenes (ginger), and aromatic aldehydes (cinnamon). Highest catalase activity (160.86 kU/g Hb) was reached in mixtures with high cinnamaldehyde and eugenol contents, whereas an antagonistic effect was observed between tea tree and geranium oils. Finally, an optimal formulation (desirability = 0.927) was identified (% *w*/*w*): 31.7% ginger, 39.1% cinnamon, 14.5% tea tree, and 14.7% geranium. Experimental validation confirmed no significant difference compared with developed predictive models. This optimized mixture constitutes a bioactive natural component with potential for use in products aimed at promoting skin health, warranting further investigation into direct models of skin healing.

**Keywords:** essential oil; mixture design; phytochemical synergy; cutaneous healing

Check for updates

Academic Editor: Sanggil Lee

Received: 2 September 2025
Revised: 21 October 2025
Accepted: 27 October 2025
Published: 5 March 2026

**Copyright:** © 2026 by the authors. Licensee MDPI, Basel, Switzerland. This article is an open access article distributed under the terms and conditions of the Creative Commons Attribution (CC BY) license.

## 1. Introduction

Increasingly, the literature recognizes plant-derived compounds' importance for pharmaceutical and cosmetic applications. This trend is driven by the consumer preference for

natural ingredients, which are perceived to have a lower incidence of adverse effects compared to synthetic counterparts, and have a long history of use in traditional medicine [1]. Consequently, essential oils (EOs), volatile and aromatic liquids extracted from various plant parts, have garnered considerable attention [2]. Historically, EOs have been employed for their aromatic, flavoring, and preservative properties [3]. However, current EO literature largely focuses on therapeutic potential. Extensive research reveals significant antimicrobial, antioxidant, and anti-inflammatory activities, plus modulation of cellular mechanisms associated with chronic diseases [4]. Scientific validation of traditional uses, coupled with demand for novel therapeutic modalities, continues to drive comprehensive study into EO chemical compositions and complex bioactivities [5]. Tissue integrity restoration after injury is a key component in skin healing. However, managing chronic wounds and associated infections present a major clinical practice problem, diminishing patients' quality of life and imposing a considerable healthcare system burden [6]. The global rise in antimicrobial resistance accentuates this problem, creating an urgent need for alternative therapeutic strategies. In this context, natural products, particularly EOs, attract considerable attention, due to a rich phytochemical composition and documented biological properties [7]. EOs' ability to simultaneously modulate multiple pathological processes—including inflammation, microbial infection, and tissue growth promotion—suggests multitarget therapeutic potential in modern wound care [8].

Essential oil from *Cinnamomum cassia* (cinnamon) stem bark contains trans-cinnamaldehyde as its principal component, contributing to a distinctive aroma and various biological activities. Studies show cinnamaldehyde exhibits neuroprotective effects against oxidative stress and apoptosis with in vitro cellular models [9]. The oil also demonstrates antifungal activity against several fungal species that are relevant to food spoilage and human health [10,11]. Documented antibacterial properties exist against foodborne pathogens and bacteria implicated in animal diseases, such as bovine mastitis and clinical endometritis in dairy cows [12]. In wound healing, *C. cassia* essential oil is a multifunctional agent. Topical application has been shown to reduce the inflammatory phase, increase fibroblast distribution and collagen deposition, and accelerate cell proliferation, re-epithelialization, and keratin synthesis [13]. At a molecular level, cinnamon oil significantly increases mRNA levels of key growth factors, including insulin-like growth factor I, fibroblast growth factor, and vascular endothelial growth factor. Upregulation of these factors—crucial mediators for angiogenesis, cell proliferation, and tissue remodeling—underscores a direct pro-regenerative role for the oil [14].

Egyptian geranium (*Pelargonium asperum*) essential oil, characterized by high citronellol and geraniol levels, has been investigated for therapeutic properties [15]. Several studies documented its anti-inflammatory, antioxidant, antibacterial, and anticancer activities [16,17]. Geranium oil reportedly inhibits the production of proinflammatory cytokines, such as tumor necrosis factor-alpha (TNF-α) and interleukin-1 beta (IL-1β), a relevant mechanism for managing inflammatory conditions [18]. Geranium oil also shows antifungal efficacy against *Candida* species and dermatophytes, highlighting potential for treating cutaneous fungal infections [19]. A key aspect is its safety profile; low toxicity and broad-spectrum antimicrobial activity render it a viable option for prolonged injury care use, minimizing the adverse reaction risk that could impede healing [20]. Furthermore, the oil exhibited synergistic antimicrobial activity with other agents like Citricidal®. This capacity is valuable in addressing increasing antimicrobial resistance, as it may improve existing treatment efficacy and reduce reliance on single-agent antibiotics [21].

Steam distillation from *Melaleuca alternifolia* (tea tree) leaves yields an essential oil recognized for broad-spectrum antimicrobial activity [22]. Its complex composition, particularly a high concentration of terpinen-4-ol, plays a key role in antibacterial, antifungal,

antiviral, and anti-inflammatory properties [23,24]. Many previous studies focused on oil efficacy against skin-infecting microorganisms, including *Staphylococcus aureus* and *Candida* species, and its potential in managing acne vulgaris and other dermatological conditions [25]. Tea tree oil holds particular interest for managing chronically infected wounds. Its primary action mechanism is microbial cell membrane disruption. Lipophilic components, particularly terpinen-4-ol, diffuse through the microbial cell membrane, disrupting the lipid bilayer. This process increases membrane fluidity and permeability, inhibits enzymes, and leads to essential metabolite leakage, ultimately causing cell death [26]. This physical action mode is particularly relevant in addressing increasing antibiotic resistance, as it is less susceptible to traditional resistance mechanisms.

Essential oil from ginger (*Zingiber officinale*) rhizomes contains high levels of volatile compounds, including zingiberene and citral [27]. Ginger and its extracted components are traditionally used in medicine, having established anti-inflammatory, antioxidant, and antiemetic effects [5,28]. Scientific investigations show that ginger essential oils exhibit antimicrobial activity against foodborne pathogenic bacteria and oral microflora [29]. Furthermore, studies investigated its potential to modulate inflammatory responses and provide protective effects against oxidative cell damage [30]. The bioactive compound 6-gingerol has been studied for anti-inflammatory and cutaneous healing properties. However, 6-gingerol has poor pharmacokinetic characteristics, including low aqueous solubility and poor bioavailability. To overcome these limitations, recent studies utilized 6-gingerol-loaded nanophytosomes. This approach demonstrated selective antiproliferative activity, significant downregulation of inflammatory markers and cytokines, and an enhanced wound-healing process [31]. Application of such novel technologies overcomes these limitations, enhancing therapeutic activity and demonstrating how pharmaceutical innovations can maximize natural compound potential [4]. It is important to note that this study serves as a foundational step. The primary objective was to utilize a "formulation by design" approach, to efficiently screen a complex, multi-component system and identify a single, optimized blend with promising bioactivity. The selected in vitro assays (photoprotection, membrane stabilization, and enzymatic antioxidant activity) were chosen as rapid, reproducible screening tools, targeting key mechanisms relevant to skin protection and repair. While these are indirect measures of the multifaceted skin-healing process, this strategy allows for the rational formulation of a candidate blend that can subsequently be validated in more complex and direct biological models. The findings are expected to contribute directly to natural product-based treatments, providing a methodological strategy and a final formulation as an active ingredient (not a finished product) for future in vitro or in vivo research within the pharmaceutical or cosmetic industries.

## 2. Materials and Methods

### *2.1. Essential Oils*

Ginger (*Zingiber officinale*), cinnamon (*Cinnamomum zeylanicum*), tea tree (*Melaleuca alternifolia*), and geranium (*Pelargonium graveolens*) essential oils were selected based on importance, reported therapeutic properties, legislation, and availability. Oils were acquired from Health & Beauty Natural Oils (HBNO, Chico, CA, USA). Composition was determined by gas chromatography (GC-FID), under the following conditions: gas chromatograph (7890, Agilent Technologies, Santa Clara, CA, USA), FID detector at 250 °C, injector at 250 °C, split ratio 1:30, 1 µL injection volume, Agilent 7683 B autosampler, DB-5MS capillary column (60 m × 0.25 mm × 0.25 µm) with a 5% diphenyl-95% dimethyl-polysiloxane stationary phase, and helium carrier gas at 1 mL/min. Oven temperature program was as follows: 45 °C to 150 °C (at 3 °C/min), then to 220 °C (at 4 °C/min), and finally to 275 °C (at 10 °C/min). Three independent essential oil samples (3 µL) were dissolved in diethyl

ether (1000 ppm). Percent composition for each component was determined by automatic peak area integration from GC-FID signal and compared against calibration curves via ChemStation® B.04.03 software (Agilent Technologies, Santa Clara, CA, USA).

### *2.2. Cytotoxicity*

An MTT assay, adapted from a previously described methodology [32], was employed to evaluate in vitro cytotoxicity. Culture medium consisted of Dulbecco's modified Eagle's medium (DMEM), supplemented with 10% fetal bovine serum (FBS), 1X trypsin, and antibiotics (100 U/mL penicillin and 0.1 mg/mL streptomycin). Fibroblasts (HDF, Detroit 551, ATCC # CCL-110) were seeded in 96-well plates at 10,000 cells per well density and allowed to adhere for 24 h at 37 °C and 5% $CO_2$ in FBS-supplemented DMEM. Subsequently, a series of six concentrations from each pure essential oil were prepared via 1:2 serial dilutions, resulting in final concentrations of 100, 50, 25, 12.5, 6.25, and 3.12 µg/mL. Each essential oil was dissolved in dimethyl sulfoxide (DMSO) to create stock solutions. These were then diluted in the culture medium to achieve the final test concentrations, ensuring that the final DMSO concentration in each well did not exceed 0.5% (*v*/*v*). Fibroblasts treated with medium containing 0.5% DMSO served as the solvent control, which was confirmed to be non-toxic in preliminary assays.

These dilutions were then added to cultured cells (100 µL/well), followed by a 24 h incubation at 37 °C and 5% $CO_2$. Following incubation, 20 µL of a 0.5 mg/mL MTT solution (3-(4,5-dimethylthiazol-2-yl)-2,5-diphenyltetrazolium bromide) was added, and plates were incubated for an additional 3 h under the same conditions. Reaction was stopped by adding 100 µL/well of a solution containing 50% isopropanol and 10% sodium dodecyl sulfate (SDS), followed by a 30 min incubation. Formazan concentration was determined spectrophotometrically, by measuring absorbance at 570 nm (Varioskan, Thermo Scientific, Waltham, MA, USA). Fibroblasts treated with dimethyl sulfoxide (DMSO) as solvent were used as control. Cytotoxicity was calculated as a viability percentage for each essential oil concentration based on the optical density (OD) obtained, relative to control cells (Equation (1)). Assays were performed in two independent experiments, with three replicates per assay. All values were normalized to the untreated control. Median inhibitory concentration ($IC_{50}$) and corresponding dose (x%) vs. viability (y%) mathematical models were calculated via GraphPad Prism® 8.0 software (GraphPad, Boston, MA, USA).

$$\% \text{ viability } = \frac{\text{OD Fibroblasts exposed to EO } - \text{ blank}}{\text{OD Fibroblasts control } - \text{ blank}} \times 100 \quad (1)$$

### *2.3. Mixture Experimental Design*

A methodological approach began with individual evaluations of four EOs, followed by assessment of their combined action via an extreme vertex mixture design. Design Expert 10® software (Stat-Ease, Minneapolis, MN, USA) generated the design, and a D-optimality criterion was adopted to minimize predicted variance throughout the experimental region. In a mixture experiment, response ($Y$) is a function of relative proportions ($x_i$) for $q$ components, constrained by $0 \leq x_i \leq 1$ and $\sum i = 1 q x_i = 1$ [33]. Consequently, a quadratic Scheffé polynomial, a model adapted to this constraint, was fitted to the data. A model expressed below related the expected response, $E(Y)$, to component proportions, considering both individual and binary interactions.

$$E(Y) = \sum_{i=1}^{q} \beta_i x_i + \sum_{1 \leq i < j \leq q} \beta_{ij} x_i x_j \quad (2)$$

where $E(Y)$: expected response; $x_i$: component $i$ proportion; $\beta_i$: linear term coefficients indicating each component's individual contribution; and $\beta_{ij}$: binary interaction term coefficients quantifying synergy ($\beta_{ij} > 0$) or antagonism ($\beta_{ij} < 0$) between components $i$ and $j$. Least squares regression was used for coefficient ($\beta$) estimation. The effects of four essential oils were studied under the following formulation constraints: minimum (0.014) and maximum (0.958) mass fraction limits. Final experimental design consisted of 22 mixtures: 18 base model points, three replicates, and one additional fitting point. The point exchange algorithm was employed to fit the polynomial statistical model. To avoid errors from density differences among essential oils, all measurements were conducted by weight (PX323, Ohaus, Parsippany, NJ, USA). Experimental units (10 g per mixture) were weighed into 15 mL amber glass vials.

Following weighing, immediate agitation was performed a 300 rpm, 30 s (vortex 3, IKA, Wilmington, NC, USA). Vials were kept sealed to prevent evaporation and stored at a regulated room temperature (24 ± 2 °C); agitation was repeated prior to each test. To identify the most therapeutically suitable mixture, promoting cutaneous lesion recovery, three response variables were evaluated: red blood cell lysis inhibition (RBL), UV-B absorption capacity (UVAC), and effect on catalase activity (CA). The selection of these assays was based on their relevance to key aspects of skin protection and cellular health. While not direct models of skin healing, they provide valuable insights into the blend's potential mechanisms of action. The red blood cell (RBC) membrane test was used as a biological model to assess the blend's cytoprotective and membrane-stabilizing capabilities against oxidative stress, a known inhibitor of the healing process. This model offers greater biological relevance than purely chemical-based antioxidant assays (e.g., DPPH). This was complemented by the catalase activity assay, specifically to investigate the blend's interaction with a crucial endogenous antioxidant enzyme. All response data were expressed as mean ± SD ($n$ = 3).

### *2.4. Red Blood Cell Lysis Inhibition (RBL)*

An in vitro assay was conducted following a modified standard method [34], using a certified erythrocyte solution from University of Antioquia's blood bank. EO mixtures were diluted with 96% absolute ethanol to a final 0.2 mg/mL concentration. Ibuprofen USP (99.82%; Sigma-Aldrich, St. Louis, MO, USA) was used as a positive control (200 µg/mL), while 0.1 M phosphate buffer ($NaH_2PO_4$-$Na_2HPO_4$ pH 7.2; Merck, Darmstadt, Germany) served as the negative control. The assay procedure combined each test solution (1 mL) with a 40% $v/v$ erythrocyte solution (0.5 mL), phosphate buffer (1 mL), and 0.45% NaCl (2 mL). The resulting mixture was incubated 30 min at 30 ± 2 °C (W270, Memmert, Schwabach, Germany) and subsequently centrifuged at 4500 rpm for 20 min (Labofuge 200, Heraeus, Hanau, Germany). Hemoglobin concentration in the resulting supernatant was quantified via spectrophotometry at 560 nm. Red blood cell lysis inhibition (%) was calculated using Equation (3).

$$\% \text{ Inhibition} = \frac{\text{Abs negative control} - \text{Abs sample}}{\text{Abs negative control}} \times 100 \quad (3)$$

### *2.5. UV-B Absorption Capacity (UVAC)*

Each EO mixture was diluted with 96% absolute ethanol to a final 0.2 mg/mL concentration. Subsequently, spectrophotometric readings were taken between 290 and 320 nm at 5 nm intervals (Genesys 20, Thermo Scientific, Waltham, MA, USA), corresponding to the UV-B radiation range that is primarily responsible for skin damage. Absolute 96% ethanol was used as an instrumental blank, with 1 cm path length quartz cuvettes (Thomas Scientific, Swedesboro, NJ, USA). UV-B absorption capacity was determined by calculating

the in vitro sun protection factor (SPF), employing Equation (4) as established in previous research [35].

$$SPF = CF \times \sum_{290}^{320} (EE\ (\lambda) \times I\ (\lambda) \times Abs(\lambda)) \quad (4)$$

Equation variables are defined as follows: CF—correlation factor (10); EE(λ)—erythemogenic effect of radiation at wavelength λ; I(λ)—solar intensity at wavelength λ; and Abs(λ)—solution absorbance at wavelength λ. Product EE(λ) × I(λ) represents the constants detailed in Table 1 [35].

**Table 1.** Spectrophotometric SPF constants.

| **λ (nm)** | 290 | 295 | 300 | 305 | 310 | 315 | 320 | ∑ |
|---|---|---|---|---|---|---|---|---|
| **EE (λ) × I (λ)** | 0.0150 | 0.0817 | 0.2874 | 0.3278 | 0.1864 | 0.0839 | 0.0180 | 1.000 |

### *2.6. Catalase Activity*

For this in vitro evaluation, a previously described methodology was used [36]. A hemolysate containing 5% *v*/*v* hemoglobin in distilled water was prepared from the erythrocyte solution; immediately before analysis, this stock solution was diluted with 50 mM potassium phosphate buffer ($KH_2PO_4$-$Na_2HPO_4$, pH 7.0) at a ratio of 80 µL of stock per 1 mL of buffer, to create a working hemoglobin solution. Essential oil (EO) mixtures were diluted 1:1 with DMSO. Final reaction mixture consisted of 2 mL 30 mM $H_2O_2$ in potassium phosphate buffer, 1 mL diluted hemoglobin solution, and 20 µL of each EO mixture sample. A blank (lacking hemoglobin and EO mixture) and a positive control (lacking only EO mixture) were prepared similarly. To determine catalase kinetics' linear portion, spectrophotometric monitoring (λ = 240 nm) was performed every 15 s for a total of 165 s (Genesys 20, Thermo Fisher). Final analysis considered only linear readings obtained within the first 30 s. Preliminary assays established that hemoglobin and $H_2O_2$ solutions are highly susceptible to degradation; therefore, to avoid interference, they were freshly prepared hourly. Reaction was initiated immediately upon the addition of $H_2O_2$. The catalase-like activity (kU/g Hb) in the presence of each essential oil mixture was calculated utilizing Equation (5), where Abs: EOs mixture absorbance (Δabs/min), E: molar extinction coefficient (43.6 $M^{-1}cm^{-1}$), Hb: hemoglobin grams (g/L), Vt: assay total volume (mL), and Vh: hemolysate volume (mL).

$$kU/g\ Hb = \frac{Abs \times 1,000,000 \times Vt}{E \times Vh \times 1000 \times Hb} \quad (5)$$

### *2.7. Essential Oils Mixture Optimization*

To optimize multiple responses simultaneously, a desirability function methodology was employed. Each individual response ($d_i$) is transformed onto a common desirability scale from zero (least desirable) to one (most desirable), reflecting an optimal range for each variable [37]. Global desirability function, $D(X)$, is calculated as the geometric mean of all transformed responses using Equation (6), where n is total number of responses considered. Should any response fall outside its defined desirability range, global desirability function ($D$) becomes zero, indicating an unacceptable condition combination. Each response's optimization objective can be set to maximize, minimize, or target a specific value. Numerical optimization process seeks factor combinations that maximize this function. A global desirability value of one represents the most favorable outcome, where resulting responses meet all established criteria. Design-Expert® 10 software (Stat-Ease, Minneapolis,

MN, USA) was utilized to identify an EO mixture with optimal combined performance across the evaluated biological activities.

$$D = (d_1 \cdot d_2 \cdot \ldots \cdot d_n)^{\frac{1}{n}} = \left( \prod_{i=1}^{n} d_i \right)^{\frac{1}{n}} \quad (6)$$

### 2.8. Optimized Mixture Validation

Experimental validation involved preparing the optimal formulation identified through the optimization procedure. This mixture, comprising a specific composition, was formulated using the same essential oils as the initial study, to ensure consistency. The optimized mixture was subsequently evaluated in triplicate for the same three response variables: catalase activity (CA), red blood cell lysis inhibition (RBL), and UV-B absorption capacity (UVAC). A one-sample *t*-test validated the optimal mixture by comparing mean triplicate experimental values for each response with the value predicted by the deterministic model. A mean comparison analysis (95.0% confidence level) was employed, using a *p*-value threshold $\leq 0.05$ to reject the null hypothesis (Mean exp = Mean pred).

### 2.9. Statistical Analysis

Results were analyzed by employing analysis of variance (ANOVA) to determine significant effects from factors (essential oils) on response variables (Design-Expert 10®, Stat-Ease, Minneapolis, MN, USA), with the significance level set at $p < 0.05$. Nonsignificant terms were removed from final predictive models for each response variable, to simplify equations in terms of actual values.

## 3. Results and Discussion

### 3.1. Essential Oils Composition

Cinnamon (*Cinnamomum zeylanicum*) oil chemical composition analysis (Table 2) revealed 50 compounds: ten most abundant components accounted for 96.26% of the total composition. Major constituents included E-cinnamaldehyde, methoxycinnamaldehyde, E-cinnamyl acetate, coumarin, benzaldehyde, α-copaene, hydrocinnamic aldehyde, phenylethyl alcohol, o-anisaldehyde, and Z-cinnamaldehyde. Results showed that the principal component was cinnamaldehyde ($C_9H_8O$; 136.2 g/mol), at a concentration of 77.56%, this value fell within the established quality standard range, 70–88% (ISO 3216:1997) [38]. High cinnamaldehyde content, an aromatic unsaturated aldehyde, is a primary contributor to cinnamon's characteristic flavor and aroma. In contrast, oil derived from cinnamon leaves consists mainly of eugenol (70–95%); this compound's absence in the analyzed sample ruled out a leaf origin [39]. Geranium (*Pelargonium graveolens*) essential oil was a complex volatile terpenic and oxygenated compound mixture. Compositional analysis showed 74 distinct compounds: 15 accounted for 84.55% of the total. A chemical profile that elucidated oxygenated monoterpene and sesquiterpene predominance. Major constituents identified were citronellol (33.6%), geraniol (15.14%), citronellyl formate (7.16%), and isomenthone (6.09%), consistent with international standards (ISO 4731:2012) [40]. Among these components, citronellol ($C_{10}H_{18}O$), a monoterpene alcohol, is also found in other essential oils like citronella (*Cymbopogon nardus*) and rose (*Rosa damascena*). This compound exists in two stereoisomeric forms, (−)-citronellol and (+)-citronellol: these configurations determine both biological activity and sensory profile [41]. Its physicochemical properties, like low density, high volatility, and nonpolar organic solvent solubility, facilitate incorporation into cosmetic and pharmaceutical formulations, and use in aromatherapy [17].

**Table 2.** Detailed chemical composition of the evaluated essential oils.

| Cinnamon | (%) | Geranium | (%) | Ginger | (%) | Tea Tree | (%) |
|---|---|---|---|---|---|---|---|
| Styrene | 0.19 | (2E)-Hexenal | 0.04 | 2-Heptanone | 0.1 | α-Thujene | 0.99 |
| α-Pinene | 0.09 | α-Pinene | 0.51 | 2-Heptanol | 0.07 | α-Pinene | 2.49 |
| Camphene | 0.06 | β-Pinene | 0.05 | Tricyclene | 0.14 | Sabinene | 0.80 |
| Benzaldehyde | 0.87 | 6-Methyl-5-heptene-2-one | 0.1 | α-Pinene | 2.10 | β-Pinene | 0.79 |
| β-Pinene | 0.03 | β-Myrcene | 0.15 | Camphene | 7.11 | β-Myrcene | 0.96 |
| Benzofuran | 0.01 | α-Phellandrene | 0.08 | Sabinene + β-Pinene | 0.35 | α-Phellandrene | 0.57 |
| Octanal | 0.01 | δ3-carene | 0.03 | Neomenthol | 0.82 | α-Terpinene | 10.55 |
| p-Cymene | 0.03 | α-Terpinene | 0.02 | β-Myrcene | 0.85 | p-Cymene | 1.75 |
| Limonene | 0.04 | p-Cymene | 0.07 | α-Phellandrene | 0.22 | β-Phellandrene + Limonene | 1.98 |
| 1.8-Cineole | 0.01 | Limonene | 0.31 | Octanal | 0.14 | 1,8-Cineole | 3.24 |
| Benzyl alcohol | 0.04 | 1,8-Cineole | 0.08 | δ3-carene | 0.04 | γ-Terpinene | 21.17 |
| Salicylaldehyde | 0.30 | (Z)-β-Ocimene | 0.06 | p-Cymene | 0.05 | cis-Sabinene hydrate | 0.08 |
| Acetophenone | 0.03 | (E)- β-Ocimene | 0.11 | Limonene + β-Phellandrene | 4.99 | α-Terpinolene | 3.87 |
| o-Guaiacol | 0.04 | cis-Linalool oxide | 0.18 | 1,8-Cineole | 2.67 | trans-Sabinene hydrate | 0.17 |
| Phenylethyl Alcohol | 0.51 | α-Terpinolene | 0.14 | γ-Terpinene | 0.03 | Linalool | 0.06 |
| ortho-vinylanisole | 0.08 | Linalool | 4.35 | α-Terpinolene | 0.18 | cis-para-Menth-2-en-1-ol | 0.35 |
| Hydrocinnamic aldehyde | 0.63 | 6-methyl-3,5-heptadien-2-one | 0.08 | trans-Linalool oxide | 0.13 | trans-p-2-Menthen-1-ol | 0.26 |
| 3-Methyl-benzofuran | 0.09 | cis-Rose oxide | 1.16 | Rosefuran | 0.12 | Terpinen-4-ol | 38.38 |
| α-Terpineol | 0.02 | trans-Rose oxide | 0.48 | Linalool | 0.22 | α-Terpineol | 2.82 |
| (Z)-Cinnamaldehyde | 0.44 | Menthone | 1.18 | 2-Nonanol | 0.04 | cis-Piperitol | 0.07 |
| Hydrocinnamyl alcohol | 0.13 | Citronellal | 0.19 | cis-para-Menth-2-en-1-ol | 0.04 | trans-Piperitol | 0.12 |
| o-Anisaldehyde | 0.50 | Isomenthone | 6.09 | trans-para-Mentha-2-en-1-ol | 0.02 | Piperitone | 0.06 |
| Phenyl ethyl acetate | 0.09 | δ-Terpineol | 0.04 | Camphor | 0.08 | δ-EIemene | 0.18 |
| (E)-Cinnamaldehyde | 77.56 | Neo-Menthol | 0.15 | Camphene hydrate | 0.06 | α-Cubebene | 0.06 |
| (E)-Cinnamyl alcohol | 0.18 | α-Terpineol | 0.32 | Isoborneol | 0.03 | Isoledene | 0.06 |
| α-Ylangene | 0.06 | Nerol | 0.22 | Citronellal | 0.06 | α-Copaene | 0.10 |
| α-Copaene | 0.73 | Citronellol | 33.6 | Borneol | 0.89 | 7-Cubebene | 0.05 |
| β-Caryophyllene | 0.14 | Neral | 0.43 | Isoneral | 0.04 | β-Elemene | 0.08 |
| Coumarin | 2.16 | Piperitone | 0.07 | Terpinen-4-ol | 0.09 | α-Gurjunene | 0.34 |
| trans-α-Bergamotene | 0.07 | Geraniol | 15.14 | Rosefuran epoxide | 0.09 | β-Caryophyllene | 0.43 |
| (E)-Cinnamyl acetate | 3.19 | Geranial | 0.73 | α-Terpineol | 0.48 | γ-Maaliene | 0.05 |
| Aromandendrene | 0.06 | Citronellyl formate | 7.16 | Myrtenal | 0.04 | β-Gurjunene | 0.02 |
| (E)-β-Farnesene | 0.02 | Geranyl formate | 2.93 | Myrtenol | 0.03 | α-Maaliene | 0.05 |
| γ-Muurolene | 0.11 | α-Cubebene | 0.17 | Decanal | 0.18 | Aromandendrene | 0.97 |
| Ar-Curcumene | 0.06 | Citronellyl acetate | 0.24 | Citronellol | 0.14 | Selina-5,11-diene | 0.14 |
| Viridiflorene | 0.08 | α-Copaene | 0.57 | Neral | 0.07 | trans-Muurola-3,5-diene | 0.17 |
| Amorphene<alpha-> | 0.10 | β-Bourbonene | 1.24 | Geraniol | 0.37 | α-Humulene | 0.07 |
| β-Bisabolene | 0.19 | Geranyl acetate | 0.47 | Geranial | 0.10 | Alloaromadendrene | 0.47 |
| trans-Calamenene | 0.03 | Phenethyl isobutyrate | 0.04 | Bornyl acetate | 0.09 | Valerena-4,7(11)-diene | 0.04 |
| δ-Cadinene | 0.19 | α-Gurjunene | 0.06 | 2-Undecanone | 0.19 | γ-Gurjunene | 0.03 |
| M-cinnamaldehyde | 9.67 | β-Caryophyllene | 1.45 | δ-EIemene | 0.12 | trans-Cadina-1(6),4-diene | 0.28 |
| (E)-α-Bisabolene | 0.05 | β-Copaene | 0.16 | Citronellol acetate | 0.17 | γ-Muurolene | 0.05 |
| Nerolidol | 0.12 | 6,9-Guaiadiene | 0.37 | Cyclosativene II | 0.10 | β-Selinene | 0.07 |
| Spathulenol | 0.10 | unknown | 0.56 | α-Copaene | 0.47 | All-Aromadendr-9-ene | 0.07 |
| Caryophyllene oxide | 0.07 | α-Humulene | 0.35 | β-Cubebene | 0.06 | trans-Muurola-4(14),5-diene | 0.08 |
| τ-Cadinol | 0.04 | Citronellyl propionate | 0.36 | β-Elemene | 1.23 | Viridiflorene + Bicyclogermacrene | 1.93 |
| α-Cadinol | 0.01 | Alloaromadendrene | 0.2 | 7-epi-Sesquithujene | 0.25 | α-Muurolene | 0.10 |
| α-Bisabolol | 0.04 | γ-Muurolene | 0.09 | β-Caryophyllene | 0.09 | γ-Cadinene | 0.04 |
| Benzyl Benzoate | 0.04 | trans-Cadina-1(6),4-diene | 0.21 | β-Copaene | 0.05 | δ-Cadinene | 1.39 |
| Phenylethyl benzoate | 0.03 | Germacrene D | 1.77 | γ-Elemene | 0.49 | trans-Cadina-1,4-diene | 0.19 |
| | | β-Selinene | 0.29 | trans-α-Bergamotene | 0.09 | Spathulenol | 0.05 |
| | | Geranyl propionate | 0.68 | Alloaromadendrene | 0.25 | Globulol | 0.20 |
| | | γ-Amorphene | 0.07 | Sesquisabinene B | 0.37 | Viridiflorol | 0.10 |
| | | Viridiflorene | 0.62 | (E)-β-Famesene | 0.39 | Cubeban-11-ol | 0.06 |
| | | α-Muurolene | 0.14 | Selina-4,11-diene | 0.16 | Eudesm-5-en-11-ol analog | 0.05 |
| | | γ-Cadinene | 0.29 | γ-Muurolene | 0.05 | Rosifoliol | 0.08 |
| | | trans-Calamenene | 0.19 | Germacrene D | 1.22 | 1-epi-Cubenol | 0.13 |
| | | δ-Cadinene | 1.31 | β-Selinene | 0.11 | Cubenol | 0.06 |
| | | trans-Cadina-1,4-diene | 0.16 | Ar-Curcumene | 7.13 | α-Muurolol | 0.02 |

**Table 2.** *Cont.*

| Cinnamon | (%) | Geranium | (%) | Ginger | (%) | Tea Tree | (%) |
|---|---|---|---|---|---|---|---|
| | | Citronellyl butyrate | 0.95 | α-Zingiberene | 33.77 | | |
| | | Geranyl butyrate | 1.15 | β-Bisabolene | 7.12 | | |
| | | Caryophyllene oxide | 0.12 | (3E,6E)- α-Farnesene | 4.03 | | |
| | | Phenylethyl tiglate | 0.82 | δ-Cadinene | 0.19 | | |
| | | 10-epi-γ-Eudesmol | 4.86 | β-Sesquiphellandrene | 12.66 | | |
| | | Geranyl iso-valerate | 0.03 | (E)-γ-Bisabolene | 0.32 | | |
| | | Cubenol | 0.08 | α-Elemol | 0.45 | | |
| | | T-Cadinol | 0.5 | Germacrene B | 0.17 | | |
| | | α-Eudesmol | 0.25 | trans-Sesquisabinene hydrate | 0.19 | | |
| | | T-MuurolоI | 0.09 | (E)-Nerolidol | 0.42 | | |
| | | Geranyl valerate | 0.17 | cis-Zingiberenol | 0.22 | | |
| | | Citronellyl tiglate | 0.29 | β-Eudesmol | 0.19 | | |
| | | α-Bisabolol | 0.08 | γ-Eudesmol | 0.15 | | |
| | | Geranyl tiglate | 1.16 | α-Eudesmol | 0.09 | | |
| | | Geranyl caprylate | 0.05 | | | | |
| Total Identified | 99.34 | Total Identified | 98.34 | Total Identified | 96.19 | Total Identified | 99.80 |

Ginger (*Zingiber officinale*) essential oil compositional analysis identified 73 distinct compounds, comprising mainly monoterpenes, sesquiterpenes, and phenolic constituents. Among these compounds, 11 represented 84.09% of the chemical composition. Major components were α-zingiberene (33.77%), β-sesquiphellandrene (12.66%), β-bisabolene (7.12%), ar-curcumene (7.13%), and camphene (7.1%). Zingiberene ($C_{15}H_{24}$; 204.18 g/mol), the predominant sesquiterpene, is fundamental to the oil's distinctive characteristics. This compound contributes significantly to the organoleptic profile, imparting warm, earthy, and spicy notes, while also contributing to the biological properties, including its anti-inflammatory, antioxidant, and antimicrobial activities. Its importance has positioned it as an essential chemotaxonomic marker for this oil's characterization [42]. Zingiberene's presence and concentration confirmed the essential oil's authenticity, ruling out potential adulterations or variations attributable to the geographical origin and extraction method. The analyzed oil complied with quality standards for its declared designation of origin and chemotype, according to ISO 16928:2014 [43]. Major components were α-zingiberene (33.77%, within the ISO standard of 23–45%) and β-sesquiphellandrene (12.66%, within the ISO standard of 8–17%).

Tea tree (*Melaleuca alternifolia*) essential oil, from this Australian native species' leaves, has a composition characterized by monoterpenes, sesquiterpenes, and terpenic alcohols. Compositional analysis identified 59 distinct compounds, 11 of which constituted 89.47% of the total oil. Major components included terpinen-4-ol (38.38%), γ-terpinene (21.17%), α-terpinene (10.55%), α-terpinolene (3.87%), and α-terpineol (2.82%). Its principal component, terpinen-4-ol ($C_{10}H_{18}O$; 154.25 g/mol), is a monoterpenoid alcohol whose structure, featuring a ten-carbon skeleton modified by a hydroxyl (-OH) group, is a key determinant of both its reactivity and biological properties [44]. Chiral centers in its structure give rise to optical isomers; their specific conformations influence interactions with biological systems and determine sensory characteristics for aromatic, cosmetic, and anesthetic applications [45]. Analyzed oil quality was verified according to the ISO 4730:2025 standard [46]. This standard establishes acceptable concentration ranges from 35 to 48% for terpinen-4-ol and 14 to 28% for γ-terpinene. Evaluated samples successfully met these established criteria for tea tree essential oils.

Quantitative analysis demonstrated distinct phytochemical profiles for each essential oil (Table 3). Monoterpenes ($C_{10}H_{16}$) are fundamental volatile compounds in essential oils, characterized by low molecular weights and high volatility. These compounds are primarily responsible for immediate olfactory impact and often contribute significantly to therapeutic properties through antimicrobial and antioxidant activities [47]. Tea tree oil exhibited the highest content among these compounds, followed by ginger, whereas

geranium and cinnamon contained substantially lower proportions. This distribution pattern suggests tea tree and ginger oils possessed more pronounced volatile profiles, potentially enhancing efficacy in applications requiring rapid aromatic impact or therapeutic action. Sesquiterpenes ($C_{15}H_{24}$), characterized by higher molecular weight and lower volatility than monoterpenes, typically contribute to fixative properties in essential oils. They often provided sustained bioactive effects over prolonged periods, demonstrating anti-inflammatory, antioxidant, and immunomodulatory properties [48]. Ginger oil showed notable sesquiterpene dominance. This significant concentration suggested suitability in applications where prolonged therapeutic effects are needed, such as anti-inflammatory or antioxidant treatments where a sustained active compound release is desirable.

**Table 3.** Comparation of the phytochemical group distribution in the evaluated essential oils.

| Group | Abbreviation | Cinnamon | Geranium | Ginger | Tea Tree |
|---|---|---|---|---|---|
| Monoterpenes | MTP | 0.25 | 1.57 | 13.91 | 44.95 |
| Oxygenated Monoterpenoids | MTPO | 0.03 | 77.32 | 6.30 | 45.61 |
| Sesquiterpenes | SQTP | 2.09 | 11.43 | 71.07 | 7.74 |
| Oxygenated Sesquiterpenes | SQTO | 0.38 | 6.38 | 2.11 | 0.75 |
| Aromatic Aldehydes | ALAR | 89.97 | 0 | 0 | 0 |
| Aromatic Alcohols | ACAR | 0.86 | 0 | 0 | 0 |
| Aromatic Esters | ESAR | 3.25 | 0.86 | 0 | 0 |
| Aliphatic Aldehydes | ALAL | 0.01 | 0.04 | 0.32 | 0 |
| Aliphatic Ketones | CEAL | 0.03 | 0.18 | 0.29 | 0 |
| Aliphatic Alcohols | ACAL | 0 | 0 | 0.11 | 0 |
| Other Non-Terpenes | ONTE | 2.57 | 0.56 | 2.08 | 0.75 |
| Unidentified | NIDT | 0.66 | 1.66 | 3.81 | 0.2 |

Oxygenated sesquiterpenoids ($C_{15}H_{24}O$), although typically present in smaller quantities than their nonoxygenated counterparts, possess biological activity and contribute to antifungal and antiallergic properties that complement essential oil therapeutic profiles [49]. Geranium oil presented the highest concentration in these compounds, followed by ginger, while tea tree and cinnamon oils contained comparatively minimal amounts. Despite a modest presence, these compounds can enhance oils' bioactive properties, particularly in geranium, where they likely contributed to efficacy [50]. Aromatic aldehydes ($C_6H_5CHO$) represented a significant nonterpenic compound class, imparting distinctive organoleptic properties. Cinnamon oil's composition was predominantly characterized by this group, which was absent in other analyzed oils. The high cinnamaldehyde concentration explained the characteristic spicy aromatic profile [51].

Aromatic alcohols ($C_6H_5CH_2OH$) and esters ($R-COO-R'$) were detected in limited quantities; cinnamon oil contained both groups, and geranium oil only esters, while both were absent in ginger and tea tree oils. Similarly, aliphatic aldehydes ($C_nH_{2n}O$), ketones ($R-CO-R'$), and aliphatic alcohols ($C_nH_{2n+1}OH$), typically found at minimal concentrations, can contribute to complex aromatic bouquets and provide synergistic effects, enhancing overall bioactivity [52]. Although ginger showed the highest levels among these trace components, they remained minor constituents across all analyzed oils, suggesting that their role in determining the predominant characteristics is negligible. The other nonterpenic compounds category includes various chemical structures that may contribute to oils' holistic properties through complex synergies. Ultimately, compositional analysis confirmed that a vast majority of components in each oil were successfully categorized into established chemical groups.

A comparative analysis identified 15 common compounds that were present in at least two of the four essential oils (Table 4). These compounds belong primarily to the terpene family (monoterpenes, sesquiterpenes) and their oxygenated derivatives. This analysis was fundamental to present work, as subsequent study stages employed mixtures combining these essential oils. While common components are not present in high concentrations within individual oils, an additive effect is anticipated upon combination. This phenomenon would increase their final concentrations in the mixtures, likely influencing biological activity parameters to be evaluated. Exhaustive characterization provided a solid basis to understand chemical mechanisms underlying therapeutic applications from these oils, both individually and in combination.

**Table 4.** Common phytochemical compounds in the essential oils studied (% *w*/*w*).

| Compound | Cinnamon | Geranium | Ginger | Tea Tree |
|---|---|---|---|---|
| α-Pinene | 0.09 | 0.51 | 2.1 | 2.49 |
| β-Pinene | 0.03 | 0.05 | 0.35 | 0.79 |
| β-Myrcene | 0 | 0.15 | 0.85 | 0.96 |
| α-Phellandrene | 0 | 0.08 | 0.22 | 0.57 |
| p-Cymene | 0.03 | 0.07 | 0.05 | 1.75 |
| Limonene | 0.04 | 0.31 | 4.99 | 1.98 |
| 1,8-Cineole | 0.01 | 0.08 | 2.67 | 3.24 |
| α-Terpinolene | 0 | 0.14 | 0.18 | 3.87 |
| α-Terpineol | 0.02 | 0.32 | 0.48 | 2.82 |
| β-Caryophyllene | 0.14 | 1.45 | 0.09 | 0.43 |
| α-Copaene | 0.73 | 0.57 | 0.47 | 0.1 |
| δ-Cadinene | 0.19 | 1.31 | 0 | 1.39 |
| Caryophyllene oxide | 0.07 | 0.12 | 0 | 0 |
| Aromandendrene | 0.06 | 0.2 | 0 | 0.97 |
| γ-Muurolene | 0.11 | 0.09 | 0 | 0.05 |

### *3.2. Cytotoxicity*

MTT assay is based on converting 3-[4,5-dimethylthiazol-2-yl]-2,5 diphenyl tetrazolium bromide into formazan crystals by living cells. As the total mitochondrial activity in most cell populations relates to viable cell numbers, this assay is widely used to measure in vitro cytotoxic effects (Figure 1). Concurrently, optical microscopy images (Figure 2) provided a visual snapshot of cytotoxic effect on cell morphology at a specific concentration. Dose–response data for the four essential oils tested against Detroit 551 fibroblasts revealed a clear hierarchy of cytotoxicity, with cinnamon being the most cytotoxic, followed by ginger, tea tree, and finally geranium, which was the least cytotoxic. At an initial 3.13 µg/mL, the oils segregated into two groups: the biocompatible geranium (96.76% viability) and tea tree (92.76%) oils, versus the more toxic ginger (82.2%) and cinnamon (77.8%) oils.

As the concentrations increased, cytotoxicity differences became more pronounced. At 50 µg/mL, cinnamon oil reduced cell viability to 17.32% and ginger oil to 26%, whereas tea tree and geranium oils preserved 50.43% and 63.52% of fibroblasts, respectively; at this concentration, ginger oil proved to be nearly twice as cytotoxic as tea tree oil. Viability ratios further quantified these disparities. At 100 µg/mL, cells treated with tea tree oil showed a viability that was 3.1-fold higher than those treated with ginger (37.25% vs. 11.92%), while geranium-treated cells had a survival rate 6.1-fold higher than cinnamon-treated cells (43.52% vs. 7.12%). Overall, cinnamon and ginger exerted the greatest cytotoxic effect, reducing viability by 91.38 and 86.58 percentage points, respectively, far exceeding the reductions from tea tree (61.25 points) and geranium (54.98 points). Collectively, these analytical approaches supported the established cytotoxic classification.

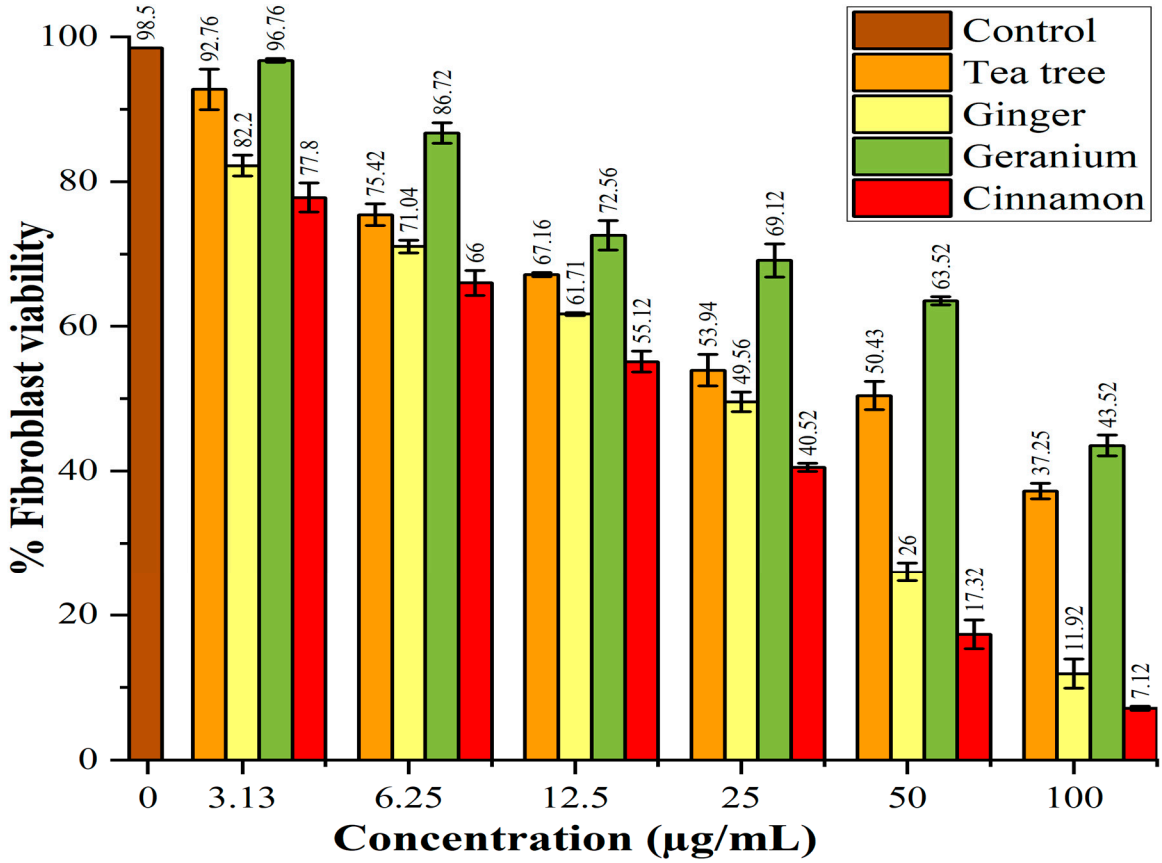



**Figure 1.** Detroit ATCC 551 skin fibroblasts viability against different essential oil concentrations.

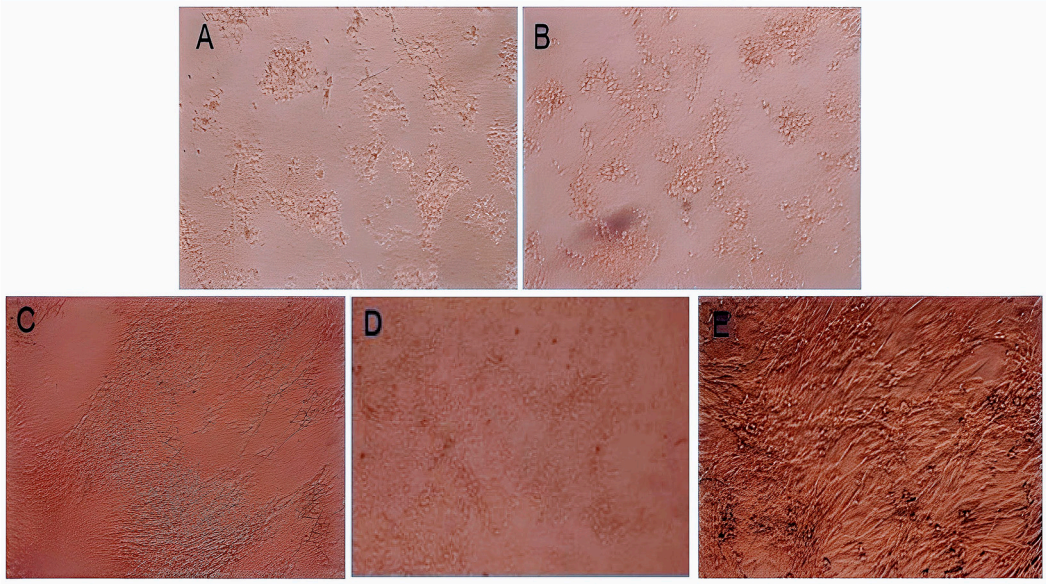



**Figure 2.** Detroit 551 ATCC fibroblasts treated with essential oils (50 µg/mL). Panels show cells treated with (**A**) tea tree, (**B**) ginger, (**C**) geranium, (**D**) cinnamon, (**E**) control. 10× optical microscopy.

Cinnamon essential oil exhibited the highest cytotoxicity with the lowest $IC_{50}$ value (21.03 ± 1.14 µg/mL), differentiating it significantly from ginger and establishing the upper extreme in the evaluated cell toxicity spectrum. A dose–response relationship (*x*% concentration vs. y% viability) was fitted to a linear model $y = 59.68 \log_{10}(x) - 28.93$ with an $R^2$ of 0.98. Cinnamon oil cytotoxic effects at a cellular level are attributed to its principal component, cinnamaldehyde, which constituted 77.56% of the EO used. Another

investigation regarding cinnamon EO cytotoxic activity found that concentrations below 100 μg/mL had a cytotoxic effect on human fibroblast cells [53]. Cinnamaldehyde disrupts cell membrane integrity and permeability, causing the loss of essential components and subsequent cell death; this effect depends on concentration, exposure time, and tissue type. Cinnamaldehyde had dual biological properties; while possessing antioxidant capacity, at high concentrations it manifested a pro-oxidant effect, generating oxidative stress. Cinnamaldehyde damages cellular structures such as proteins, lipids, and DNA, and its mechanism involves inhibiting cellular ATPase, which diminishes the electrochemical gradient that is necessary for nutrient absorption and leads to osmotic collapse [53]. Cinnamaldehyde's cytotoxic effect was dose and time-dependent in HSC3 cells, with a reported $IC_{50}$ of 10 μg/mL and significant documented morphological changes in treated cells [54]. Consistent with these findings, the present study's observations revealed that cinnamon oil (Figure 2D) was the most aggressive agent, causing nearly total cell monolayer destruction. The microscopic field appeared devoid of adhered cells, confirming an extremely high cytotoxicity degree.

With an $IC_{50}$ of 41.67 ± 3.86 μg/mL, tea tree essential oil exhibited intermediate cytotoxicity (Figure 1). Data analysis indicated that cell viability decreased proportionally with increasing oil concentration, following a linear model $y = 39.02 \log_{10}(x) - 12.51$ ($R^2 = 0.96$). While generally considered safe for topical application, tea tree oil can cause skin irritation and allergic reactions, particularly at high concentrations (>25%) or when degraded by oxidation from prolonged light and air exposure [55]. Observed cytotoxic effects can be explained by a synergy of biochemical mechanisms affecting membrane structural integrity and energetic and genomic homeostasis. These effects, documented in bacterial, fungal, and eukaryotic models [55], are dose-dependent and mediated by the oil's terpene-rich composition, including components like terpinen-4-ol (38.38%) and 1,8-cineole (2.82%) that are present in the used oil. Reports also indicate that 1,8-cineole, a minor identified component, inhibits aminoacyl-tRNA synthetase in HeLa cells, thereby blocking tRNA-loading with amino acids and halting peptide elongation; terpinen-4-ol potentiates this effect, interfering with the 80S ribosome structure by binding to the 60S subunit [44]. Specifically in human fibroblasts, 24 h of exposure to 0.1% tea tree oil reportedly induces cytoplasmic vacuolization and plasma membrane phospholipid asymmetry loss [56]. The present study's results showed that tea tree oil demonstrated moderate cytotoxic effects, although less extreme than cinnamon and ginger at the same concentration. A reduction in viable, adhered cell numbers was observed compared to control. Remaining cells lost their characteristic fusiform morphology, adopting a rounded shape indicative of cellular stress, death, or detachment (Figure 2A).

Ginger essential oil had the second highest cytotoxic level, evidenced by a high $IC_{50}$ value (25.3 ± 1.07 μg/mL). These toxic effects from this oil can be explained through several interconnected cellular mechanisms. Major lipophilic components in this oil (α-zingiberene, 33.77%; β-sesquiphellandrene, 12.66%) readily penetrate cell membranes, altering their structural integrity and increasing permeability, leading to cell death. This membrane disruption acts in conjunction with the oil's capacity to induce oxidative stress, triggering reactive oxygen species (ROS) production and cumulative oxidative damage to cellular structures and functions [57]. A linear fit from these data yielded model $y = 59.79 \log_{10}(x) - 34.00$, with a 0.92 coefficient of determination ($R^2$), demonstrating a direct correlation between ginger oil concentration and decreased cell survival. Microscopic evaluation revealed that ginger oil (Figure 2B) induced clear cytotoxic effects at a 50 μg/mL concentration, although the effects were less extreme than those observed for cinnamon. A significant reduction in viable, adhered cell numbers was noted compared to control. These effects can be attributed to oil's interference with mitochondrial function,

disrupting ATP synthesis and activating apoptotic pathways. Furthermore, components present in ginger oil, like β-bisabolene and ar-curcumene, inhibit key cellular enzymes, thereby compromising metabolic processes essential for cell survival [58]. Underlying mechanisms induce a cascade of morphological transformations; exposed cells initially contract and round up due to cytoskeletal collapse, followed by membrane bleb formation. Significant nuclear alterations, including chromatin condensation and nuclear fragmentation, subsequently occur; this process culminates in apoptotic body formation—vesicles containing cellular components destined for phagocytosis [59].

Geranium essential oil exhibited the lowest cytotoxicity ($IC_{50}$ = 92.51 ± 8.87 µg/mL). Given its widespread use on skin, geranium oil's toxicity to normal cell lines, including fibroblasts, has been a focal point for research. Studies suggest geranium oil and its components are generally low in toxicity [17]. Previous studies, for example, show pure citronellol does not exhibit evident cytotoxic effects on fibroblast cells, with cell viability remaining above 70% (indicating a lack of toxicity per ISO 10993-5 standard) [60,61]. Notably, while citronellol was the main component (33.6%) in the oil used, it was evaluated as part of the whole essential oil, not in its pure state, which may account for observed cytotoxicity. Geranium oil's tested dose ($x$% concentration) versus viability (y%) relationship was fitted to the linear regression $y = 40.58 \log_{10}(x) - 29.51$ with $R^2 = 0.97$. Geraniol (15.14% in our study) also has low cell toxicity; studies indicate that its safety for cosmetic applications and its antioxidant properties, like reducing nitric oxide production and inflammation, suggest a protective rather than toxic effect [62]. A visual evaluation of geranium oil's cytotoxic activity revealed reduced cell death, with only a few affected cells remaining (Figure 2C). Low concentrations reported no significant cellular morphological alterations from geranium oil. While it might induce subtle, reversible membrane stress upon agent removal, beneficial effects like increased collagen and hyaluronic acid secretion by fibroblasts have also been suggested [63].

Control culture (Figure 2E) served as a baseline reference, showing a dense, healthy cell population. The cells displayed typical elongated, fusiform fibroblast morphology, were well adhered to the surface, and formed a nearly confluent monolayer. Compared with more potent essential oils, control had only minor effects and cells retained their elongated shape and remained adhered. Results indicate that, at concentrations used, this solvent (DMSO) possesses limited intrinsic cytotoxicity and was not primary driver of drastic effects observed in other treatments. In summary, qualitative visual analysis confirmed a cytotoxicity spectrum where cinnamon oil was the most potent, followed by ginger, tea tree, and geranium. This hierarchy was aligned with quantitative MTT evaluation. The evident cytotoxic potential exhibited by all pure essential oils, albeit to varying degrees, limits direct application in topical formulations. Such use is constrained by the risk of damage to healthy tissue or interference with biological processes like wound healing. Therefore, it is recalled that this work seeks to develop an active ingredient (mixture) that should be incorporated as part of a finished product.

The evident cytotoxic potential exhibited by the pure essential oils is a critical finding that informs their practical application. It is essential to distinguish between the properties of these pure, concentrated raw materials and the intended use of the final optimized blend. The cytotoxicity assays were performed to characterize the dose-dependent toxicity of each individual component, establishing a baseline for safety and understanding their intrinsic potency. However, the optimized mixture developed in this work is intended to function as a potent active ingredient, not as a finished topical product. In its final application, this blend would be incorporated at a low, non-cytotoxic concentration into a suitable dermatological carrier (e.g., a cream, ointment, or gel). Therefore, future studies must focus on determining the therapeutic window of the optimized blend—the concentration range

where it exhibits beneficial, pro-regenerative activities without inducing harm to fibroblasts or other skin cells.

### *3.3. Mixture Experimental Design*

Table 5 presents the experimental design and corresponding results from tests conducted with four essential oils. The design was structured to correlate the response variable with each component's proportion by fitting a Scheffé-type polynomial model.

**Table 5.** D-optimal mixture design and corresponding experimental results (mean ± SD) for the evaluated essential oils.

| Mixture | Essential Oil Proportion | | | | Response | | |
|---|---|---|---|---|---|---|---|
| | Ginger | Cinnamon | Tea Tree | Geranium | UVAC | RBL | CA |
| | $x_1$ | $x_2$ | $x_3$ | $x_4$ | SPF | % Inhibition | kU/g Hb |
| 1 | 0.014 | 0.486 | 0.486 | 0.014 | 4.5 ± 0.11 | 86.7 ± 2.35 | 131.87 ± 1.62 |
| 2 | 0.329 | 0.329 | 0.013 | 0.329 | 4.5 ± 0.09 | 98.1 ± 1.94 | 147.58 ± 2.91 |
| 3 | 0.014 | 0.343 | 0.329 | 0.314 | 4.4 ± 0.04 | 91.3 ± 2.58 | 124.43 ± 2.19 |
| 4 | 0.014 | 0.014 | 0.958 | 0.014 | 1.1 ± 0.05 | 95.6 ± 1.87 | 137.29 ± 3.53 |
| 5 | 0.958 | 0.014 | 0.014 | 0.014 | 1.1 ± 0.03 | 87.9 ± 2.61 | 130.43 ± 3.88 |
| 6 | 0.014 | 0.343 | 0.329 | 0.314 | 4.3 ± 0.13 | 96.1 ± 2.91 | 127.10 ± 3.75 |
| 7 | 0.014 | 0.958 | 0.014 | 0.014 | 4.5 ± 0.08 | 81.7 ± 1.29 | 160.86 ± 2.48 |
| 8 | 0.486 | 0.014 | 0.014 | 0.486 | 1.2 ± 0.02 | 95.7 ± 1.93 | 117.92 ± 2.31 |
| 9 | 0.014 | 0.486 | 0.014 | 0.486 | 4.5 ± 0.18 | 95.9 ± 2.81 | 137.01 ± 3.42 |
| 10 | 0.486 | 0.014 | 0.486 | 0.014 | 1.1 ± 0.01 | 95.5 ± 0.99 | 153.86 ± 1.58 |
| 11 | 0.014 | 0.014 | 0.014 | 0.958 | 1.2 ± 0.06 | 95.7 ± 0.93 | 135.48 ± 1.39 |
| 12 | 0.314 | 0.343 | 0.329 | 0.014 | 4.3 ± 0.07 | 96.5 ± 1.79 | 152.77 ± 2.59 |
| 13 | 0.314 | 0.343 | 0.329 | 0.014 | 4.3 ± 0.14 | 97.6 ± 2.94 | 145.38 ± 3.31 |
| 14 | 0.142 | 0.286 | 0.286 | 0.286 | 4.3 ± 0.10 | 96.1 ± 0.98 | 139.59 ± 1.45 |
| 15 | 0.157 | 0.643 | 0.029 | 0.171 | 4.5 ± 0.15 | 95.9 ± 1.75 | 147.67 ± 3.41 |
| 16 | 0.142 | 0.286 | 0.286 | 0.286 | 4.2 ± 0.12 | 96.4 ± 1.85 | 138.50 ± 2.97 |
| 17 | 0.142 | 0.286 | 0.286 | 0.286 | 4.3 ± 0.16 | 97.1 ± 2.83 | 146.03 ± 3.25 |
| 18 | 0.014 | 0.014 | 0.486 | 0.486 | 1.1 ± 0.05 | 81.2 ± 1.12 | 112.65 ± 2.68 |
| 19 | 0.129 | 0.129 | 0.142 | 0.600 | 3.1 ± 0.09 | 98.4 ± 1.98 | 134.21 ± 3.07 |
| 20 | 0.486 | 0.486 | 0.014 | 0.014 | 4.5 ± 0.17 | 92.9 ± 2.74 | 144.22 ± 2.79 |
| 21 | 0.329 | 0.013 | 0.329 | 0.329 | 1.1 ± 0.04 | 96.1 ± 1.90 | 144.30 ± 2.85 |
| 22 | 0.129 | 0.129 | 0.613 | 0.129 | 3.0 ± 0.11 | 97.3 ± 1.88 | 140.29 ± 3.65 |

A mass balance was performed for each experimental mixture, based on the phytochemical group percentage distribution in source oils (Table 3), establishing a direct connection between source essential oils (e.g., ginger and cinnamon) and underlying blend chemical composition. Observed therapeutic response differences are ultimately due to varying proportions of these phytochemical groups. Each group's proportion knowledge enables an investigation into whether the observed effects are from individual components or, more likely, from synergistic or antagonistic interactions in complex systems like essential oils. When a specific mixture shows noteworthy therapeutic activity, Figure 3 allows identifying its particular "*phytochemical fingerprint*" (e.g., high sesquiterpenes, low aromatic aldehydes). Such characterization is essential to explain which compounds are responsible for observed activity and to ensure experimental reproducibility, as it defines each experimental point's exact composition.

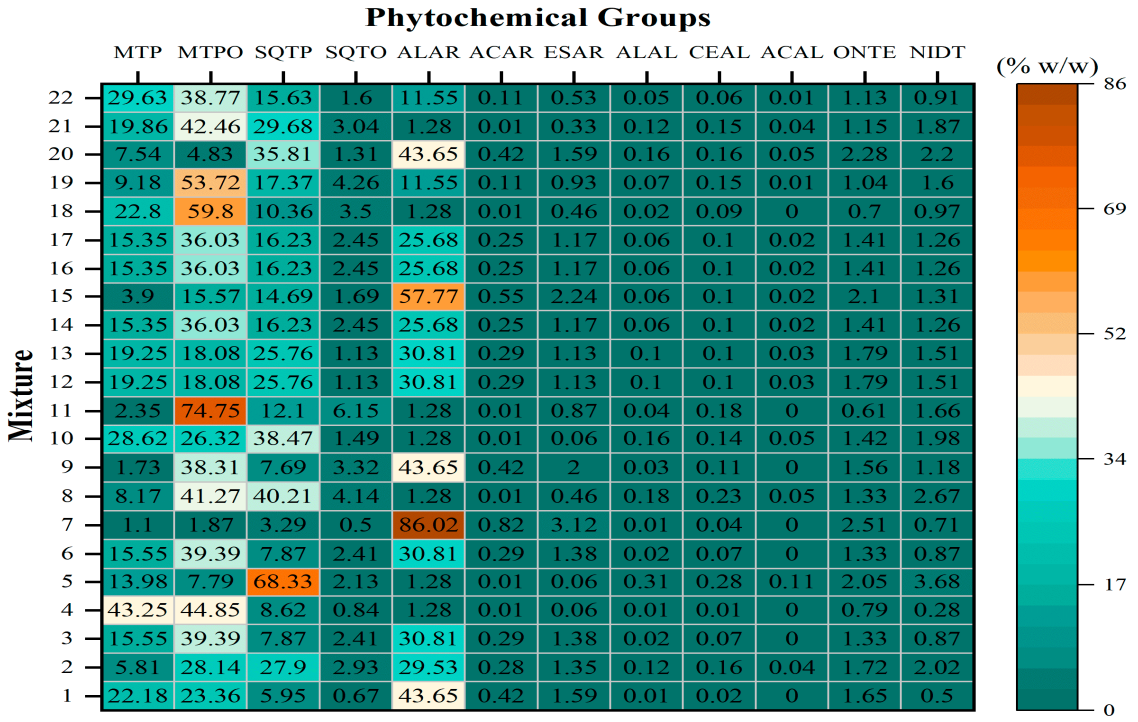



**Figure 3.** Phytochemical groups in the evaluated essential oil mixtures (% *w*/*w*). For abbreviations, see Table 3.

### *3.4. UV-B Radiation Absorption Capacity*

Solar radiation encompasses a broad electromagnetic spectrum; ultraviolet (UV) radiation is a particularly energetic portion with significant biological implications. UV spectrum is subdivided into three main regions, based on wavelength: UVC (100–280 nm), UVB (280–315 nm), and UVA (315–400 nm). Although partially filtered by atmosphere, UVB radiation reaches Earth's surface and primarily affects the epidermis—skin's most superficial layer. It is the primary cause of sunburn (erythema), tans, and plays a crucial role in developing various cutaneous diseases [64]. Chronic, unprotected UV radiation exposure is a primary risk factor for developing melanoma and other skin cancers, in addition to accelerating the cutaneous aging process [65]. Understanding how different natural compounds, such as essential oils, interact with these wavelengths is fundamental to developing effective photoprotective strategies.

Ultraviolet B radiation absorption capacity (UVAC), quantified as sun protection factor (SPF) in the experimental design (Table 5), is a fundamental variable discerning photoprotective potential of essential oil blends. Data examination revealed considerable SPF variability, with values ranging from 1.1 to 4.5 across 22 studied formulations. Several mixtures exhibited high UVAC, achieving SPF values between 4.3 and 4.5 (mixtures 1–3, 6, 7, 9, 12–17, and 20). Preliminary observations from these formulations suggest that significant cinnamon essential oil presence, either as a predominant component or in key combinations, is a common factor. In contrast, mixtures 4, 5, 8, 10, 11, and 18 presented the lowest UVAC values (SPF $\approx$ 1.1–1.2). Specifically, mixture 4 (high tea tree proportion) and mixture 5 (high ginger proportion with minimal cinnamon) both registered an SPF of 1.1, whereas mixture 11 (dominated by geranium oil) had an SPF of 1.2. Mixtures 19 and 22 were positioned in an intermediate range, with SPF values of 3.0–3.1.

Analysis of variance (ANOVA) (Table 6) confirmed overall model significance, linear mixture effect, and ginger · cinnamon ($x_1 \cdot x_2$), cinnamon · tea tree ($x_2 \cdot x_3$), and cinnamon · geranium ($x_2 \cdot x_4$) interactions. Results indicate that cinnamon's efficacy is modulated by tea tree and geranium, leading to nonadditive effects. Blends like mixture

3 (SPF 4.4), for example, demonstrate how cinnamon maintains a high SPF, even when not the majority component. Conversely, interactions not involving cinnamon were not significant, suggesting that without cinnamon's predominant influence, no notable combined UVAC effects occurred.

**Table 6.** Analysis of variance for UV-B absorption capacity of evaluated essential oil mixtures.

| Source | Sum of Squares | df | Mean Square | F-Value | *p*-Value |
|---|---|---|---|---|---|
| Model | 46.86 | 9 | 5.21 | 33.78 | <0.001 |
| Linear mixture | 32.68 | 3 | 10.89 | 70.67 | <0.001 |
| $x_1{}^*x_2$ | 4.17 | 1 | 4.17 | 27.07 | 0.002 |
| $x_1{}^*x_3$ | 0.05 | 1 | 0.05 | 0.33 | 0.528 |
| $x_1{}^*x_4$ | 0.09 | 1 | 0.09 | 0.60 | 0.445 |
| $x_2{}^*x_3$ | 5.97 | 1 | 5.97 | 38.74 | <0.001 |
| $x_2{}^*x_4$ | 4.63 | 1 | 4.63 | 30.06 | 0.001 |
| $x_3{}^*x_4$ | 0.10 | 1 | 0.10 | 0.67 | 0.336 |
| Lack of fit | 1.84 | 8 | 0.229 | 78.78 | 0.400 |
| Total | 48.71 | 21 | | | |

To quantify factor and interaction effects, a predictive statistical model for UV-B absorption capacity was developed (Equation (7)), yielding an $R^2$ coefficient of 95.5% and indicating a suitable fit with the experimental data. Calculated coefficients reinforced previous interpretations: cinnamon essential oil has the highest positive linear component, confirming its predominant impact on increasing SPF. While coefficients for ginger, tea tree, and geranium are also positive, indicating individual contributions to UVAC increase, they are of a smaller magnitude than cinnamon's. All interaction terms involving cinnamon had positive coefficients, with the cinnamon · tea tree synergism being particularly significant. These values are consistent with ANOVA results and suggest that cinnamon not only contributes to its own high absorption capacity, but also interacts synergistically with other oils, increasing SPF beyond a simple sum of their individual effects. Figure 4 illustrates the model generated from Equation (7), showing essential oils' relative proportion influence on sun protection factor (SPF) while holding ginger content constant at 0.014. Such graphical representations are important mixture design tools, allowing intuitive visualization of how a response variable, in this case SPF, is modified across a continuous component combination range.

$$\begin{aligned}\text{UVAC (SPF)} = {} & 0.773{\cdot}\textit{Ginger} + 3.869{\cdot}\textit{Cinnamon} + 0.835{\cdot}\textit{Tea Tree} + 0.985{\cdot}\textit{Geranium} + \\ & 9.438{\cdot}(\textit{Ginger}{\cdot}\textit{Cinnamon}) + 10.545{\cdot}(\textit{Cinnamon}{\cdot}\textit{Tea Tree}) + 9.673{\cdot}(\textit{Cinnamon}{\cdot}\textit{Geranium})\end{aligned} \quad (7)$$

Cinnamon essential oil emerged as a primary factor driving UV-B absorption, an effect attributed to its high aromatic aldehyde (ALAR) content, constituting 89.97% composition (Table 3). (E)-Cinnamaldehyde was the major component within this group, at 77.56% (Table 2). Cinnamon oil UV absorption is strongly influenced by its major components, particularly those with aromatic and conjugated systems. Chemically, (E)-cinnamaldehyde is an α,β-unsaturated aromatic aldehyde; its structure acts as a potent chromophore. Its aromatic ring and aldehyde carbonyl (C=O) group are conjugated via a carbon–carbon double bond (C=C), creating a delocalized π-electron system [66]. Such conjugation decreases the energy required for electronic transitions (primarily $\pi \rightarrow \pi^*$), shifting maximum absorption (λmax) to longer wavelengths (a bathochromic effect), and often increasing $n \rightarrow \pi^*$ transition intensity into UVB and low UVA regions (λmax ≈ 282–287 nm). Compounds that are structurally similar to cinnamaldehyde, like the widely used synthetic UV filter octyl methoxycinnamate, share effective UVB absorption capacity because of their conjugated

aromatic system [67]. Cinnamaldehyde's chemical properties directly explained the high UVB-AC observed in mixtures with a large cinnamon proportion. Figure 3 corroborates this conclusion, showing that mixtures with highest SPFs, such as 7 and 20, also have the highest ALAR concentrations (86.02% and 43.65%, respectively).

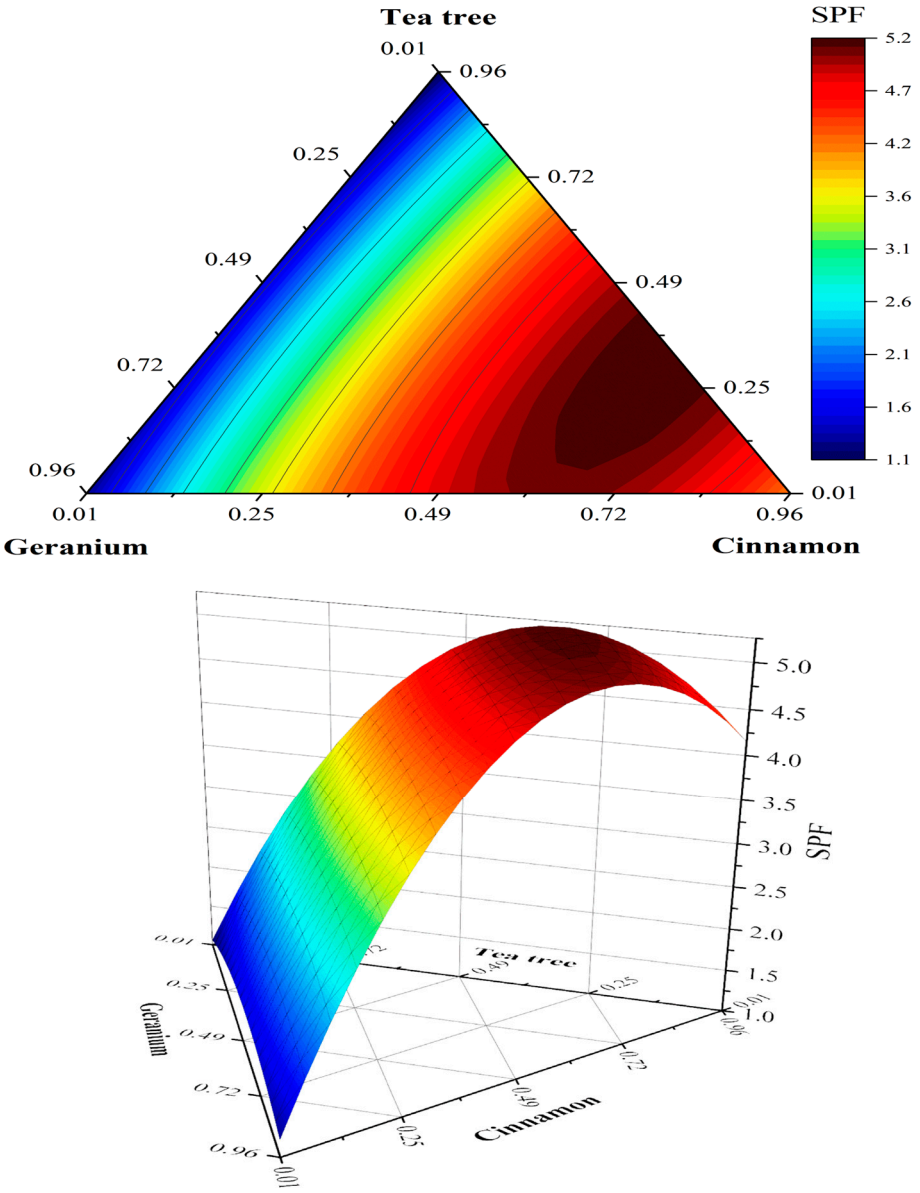



**Figure 4.** Ternary plot (**top**) and response surface (**bottom**), showing the essential oil mixtures' effect on sun protection factor (SPF). Ginger proportion constant at 0.014.

Ginger essential oil, characterized by a high sesquiterpene (SQTP) content (71.07%, Table 3), like α-zingiberene (33.77%) and β-sesquiphellandrene (12.66%) (Table 2), presented a particular UV absorption profile. Conjugated diene systems within α-zingiberene and β-sesquiphellandrene have λmax values of 232 nm and 235 nm, respectively [68]. These wavelengths fall predominantly in UVC and low-UVB regions, limiting oil's capacity for effective absorption in the more critical mid-to-high UVB range (290–320 nm). Although Ar-curcumene (7.13%), an aromatic sesquiterpene, can contribute to absorption at approximately 250–280 nm, its low concentration and molar absorptivity limit its overall impact. While ginger oil's individual contribution to UVB protection appears limited, its performance in mixtures suggests a synergistic role. Mixture 20, for example, with high, equitable proportions of ginger and cinnamon (35.81% SQTP and 43.65% ALAR), achieved

a high SPF (Figure 3). In contrast, mixture 5, high in ginger but low in cinnamon, had a limited SPF (1.1), suggesting ginger, while not a primary photoprotective agent, may interact positively or synergistically with cinnamon. The absence of phenolic compounds like eugenol also restricts oils' absorption potential around the 280 nm region, where many phenols are active. Therefore, ginger oil's contribution to photoprotection may derive more from antioxidant properties than from robust, direct UV absorption in the most critical spectral range for sun protection.

Tea tree essential oil, composed mainly from oxygenated monoterpenoids (MTPO), like terpinen-4-ol (38.38%, Table 2), and a significant monoterpene (MTP) fraction, including γ-terpinene (21.17%) and α-terpinene (10.55%) (Tables 2 and 3), derives UV absorption capacity from terpenes with conjugated double bonds. Oil's main component, terpinen-4-ol, plays a minor role in this absorption. As a monoterpenic alcohol with only a single, isolated double bond, terpinen-4-ol requires high energy for π→π* electron excitation; consequently, its principal UV absorption occurs at short wavelengths (<220 nm) [66]. This spectral region has limited cutaneous photoprotection relevance, as most UVC radiation is filtered by atmosphere. In contrast, α-terpinene and γ-terpinene are structurally more significant for UVB absorption, as both contain a 1,3-cyclohexadiene system. Double bond conjugation in this cyclic system allows for greater π-electron delocalization, reducing π→π* transition energy and causing a bathochromic shift in the main absorption band. Specifically, α-terpinene shows significant absorption in the 230–290 nm range, thereby covering a UVB band portion. Additionally, p-cymene (1.75%, Table 2), an aromatic monoterpene, contributes to mid-UVB region absorption (typically 260–270 nm), owing to characteristic electronic transitions in its benzene ring [68]. Tea tree oil's chemical profile aligns with present study results, as mixture 4, dominated by tea tree oil with minimal cinnamon content (1.28% ALAR, Figure 3), presented a low SPF.

Similarly, geranium essential oil, rich in MTPO at 77.32% (Table 3) and containing citronellol (33.6%) and geraniol (15.14%) as main components (Table 2), exhibits inherently low UV absorption capacity in the relevant photoprotective range (UVB/UVA). Its limited absorption is based on its major components' molecular structure. Citronellol, an acyclic monoterpenic alcohol, possesses only a single, isolated double bond; such a simple chromophore requires high energy for the π→π* transition, resulting in principal absorption at very short wavelengths (expected below 220 nm). Although the structurally similar geraniol contains two double bonds, they are not arranged in an extended conjugation permitting significant electron delocalization; consequently, its λmax has been reported in the 190–195 nm range, with no significant absorption above 290 nm [68]. Mixture 11, high in geranium with a minimal cinnamon proportion (1.28% ALAR, Figure 3), yielded an SPF of 1.2. Similarly, results from other mixtures dominated by geranium or tea tree with scarce cinnamon (e.g., mixtures 4 and 5) consistently underscore a lower intrinsic contribution from these oils to UVAC than cinnamon. Their limited contribution is a direct result of major components lacking chromophores that are essential for efficient UVB and UVA absorption, such as extended conjugation systems or significantly functionalized aromatic rings.

Literature confirms that cinnamaldehyde is the primary photoprotective agent, with a highly concentration-dependent SPF. Reported cinnamon SPF values range from ~3.5 in dilute extracts to 25.0 in 10% essential oils, and can exceed 100 for the isolated compound [69]. The maximum mixture's SPF of 4.5 is thus plausible for a dilute formulation. However, these data highlight the "cinnamon paradox": concentrations required for high photoprotection are unsafe for dermal application. The limited SPF from tea tree and geranium oils (~1.1–1.2 with the major component) likely stems from the lack of effective chromophores in their main constituents (e.g., terpinen-4-ol, citronellol). This conclusion aligns with

published data reporting low SPF values for both tea tree oil (~2) and geranium oil (~6.5), which are insufficient for primary sun protection [70,71]. Ginger oil's low SPF (~1.1) is likely due to its major sesquiterpenes absorbing outside the critical UVB range, a finding consistent with reports of SPF values below two for standard ginger extracts [72].

In general, cinnamon essential oil proved to be the most influential in achieving high UV-B absorption capacity (UVAC). Cinnamaldehyde's chemical structure, characterized by extended electronic conjugation, is ideal for efficient UVB region photon absorption. While ginger oil's primary absorption occurs at relatively short wavelengths, its positive cinnamon interaction suggests an additive effect, meriting further investigation into its precise mechanism. Potential synergy could involve stabilizing cinnamon chromophores or affecting blend matrix. Conversely, tea tree and geranium oils demonstrated limited individual UVAC contributions, a finding explained by major components' lack of chromophores with strong UVB-absorbing structures. Despite this, statistically significant cinnamon oil interactions imply a modulatory role. Although not primary photoprotective agents, these oils appear to enhance mixture efficacy, possibly by altering the formulation matrix, active component solubility, or by contributing to minor absorption in different UV subregions. Analysis ultimately confirmed that aromatic aldehyde (ALAR) concentration was the key and most direct SPF predictor.

### *3.5. Red Blood Cell Lysis Inhibition(RBL)*

Erythrocyte membrane, a highly organized lipoprotein structure, is susceptible to oxidative damage. Such damage can destabilize the lipid bilayer, leading to hemolysis or cell rupture. In vitro hemolysis, induced by agents like hydrogen peroxide or osmotic stress, serves as a common model for evaluating natural compounds' antioxidant and membrane stabilizing capacity. A substance's ability to protect erythrocytes from lysis is a robust indicator of cytoprotective potential, as it reflects lipid bilayer-level interactions preventing cell damage. Red blood cell lysis inhibition (RBL) by essential oil blends is therefore fundamental in determining bioactivity and elucidating action mechanisms at the cell membrane.

Experimental design data (Table 5) revealed marked RBL variability, with values fluctuating between 81.1% and 98.4% across 22 evaluated mixtures. This wide range suggests a blend's specific composition and relative proportions are key determinants in protecting the erythrocyte membrane. Mixtures 2, 19, and 22 were particularly noteworthy, exhibiting highest inhibition percentages at 98.1%, 98.4%, and 97.3%, respectively. Preliminary observations indicate that high formulation efficacy stems not from a single oil's dominance but from complex, synergistic combinations. Mixture 19, for example, the most effective, contains geranium as its main component, but also includes significant proportions from the other three oils. In contrast, mixtures 7 and 18 registered the lowest protective activity, with RBL values at 81.7% and 81.1%, respectively. Notably, mixture 7 consists almost entirely of cinnamon oil, whereas mixture 18 is a geranium and tea tree combination with minimal content from the other two oils.

Analysis of variance (ANOVA, Table 7) confirmed model's statistical significance, indicating a causal relationship between mixture composition and lysis inhibition. Importantly, the linear mixture term was not significant, demonstrating that individual additive contributions from each oil are not the primary factor governing this activity. Instead, analysis revealed that synergistic interactions between oil pairs are the determining factor. Significant binary interactions identified were cinnamon · geranium ($x_2 \cdot x_4$), ginger · cinnamon ($x_1 \cdot x_2$), and tea tree · geranium ($x_3 \cdot x_4$). This result is pivotal, confirming that erythrocyte membrane stabilization is enhanced through synergistic mechanisms and underscoring simple additive models' inadequacy for predicting complex phytochemical mixture efficacy.

**Table 7.** Analysis of variance for the effect of evaluated essential oils on red blood cell lysis. inhibition.

| Source | Sum of Squares | df | Mean Square | F-Value | *p*-Value |
|---|---|---|---|---|---|
| Model | 419.50 | 9 | 46.61 | 5.04 | 0.005 |
| Linear mixture | 42.53 | 3 | 14.18 | 1.53 | 0.256 |
| $x_1$*$x_2$ | 100.74 | 1 | 100.74 | 10.90 | 0.006 |
| $x_1$*$x_3$ | 53.46 | 1 | 53.46 | 5.79 | 0.033 |
| $x_1$*$x_4$ | 37.45 | 1 | 37.45 | 4.05 | 0.067 |
| $x_2$*$x_3$ | 8.86 | 1 | 8.86 | 0.95 | 0.346 |
| $x_2$*$x_4$ | 125.23 | 1 | 125.23 | 13.55 | 0.003 |
| $x_3$*$x_4$ | 79.96 | 1 | 79.96 | 8.65 | 0.012 |
| Lack of fit | 98.61 | 8 | 12.33 | 4.02 | 0.097 |
| Total | 530.38 | 21 | | | |

A developed polynomial regression model (Equation (8)), characterized by an $R^2$ of 93.20%, as illustrated in Figure 5, was used to quantify the relationship between essential oil mixture composition and erythrocyte lysis inhibition. Model parameters indicate that all four evaluated oils—ginger, cinnamon, tea tree, and geranium—contribute to anti-hemolytic activity, as evidenced by their positive linear coefficients. An analysis of these coefficient magnitudes establishes an intrinsic efficacy hierarchy, positioning tea tree and geranium as agents with highest individual activity, followed by ginger and cinnamon. In addition to linear effects, the model also elucidates nonadditive relations among components. Positive relationship coefficients, indicative of synergy, were observed for the ginger · cinnamon and cinnamon · geranium combinations.

A particularly relevant finding was the negative coefficient for the tea tree · geranium pair. A negative parameter indicates clear antagonism between the two most individually active components, implying that their combination results in lower total protective efficacy than a sum of separate effects. These observations have direct implications for optimized formulation design. The model predicts a strategy based solely on combining the most individually potent agents that would be suboptimal, owing to the antagonistic effect. Instead, it is postulated that maximum anti-hemolytic activity could be achieved by combining a high-efficacy component (geranium), with one exhibiting synergistic interaction, like cinnamon. The model, therefore, serves as a fundamental predictive tool guiding multicomponent mixture formulation, transcending additive assumptions while avoiding antagonistic interactions.

$$\begin{aligned}\text{RBL (\% inhibition)} = {} & 86.486 \cdot \textit{Ginger} + 80.839 \cdot \textit{Cinnamon} + 97.385 \cdot \textit{Tea Tree} \\ & + 96.539 \cdot \textit{Geranium} + 35.646 \cdot (\textit{Ginger} \cdot \textit{Cinnamon}) + 13.539 \cdot (\textit{Ginger} \cdot \textit{Tea Tree}) \\ & + 31.047 \cdot (\textit{Cinnamon} \cdot \textit{Geranium}) - 69.981 \cdot (\textit{Tea Tree} \cdot \textit{Geranium})\end{aligned} \quad (8)$$

Geranium essential oil, with citronellol (33.6%) and geraniol (15.14%) as primary MTPO, appears to play a central role in red blood cell membrane protection. These monoterpene alcohols are amphipathic compounds featuring a polar hydroxyl (-OH) head and a nonpolar terpene tail. This structure allows effective intercalation into the erythrocyte lipid bilayer, where they can modify membrane biophysical properties, like fluidity and phospholipid acyl chain order, resulting in increased mechanical resistance to lysis [73]. Biophysical studies demonstrate that geraniol can induce more ordered membrane lipid packing, decreasing fluidity within the hydrophobic core, and thereby reducing hemolytic agent permeability and preventing osmotic lysis [74]. Additionally, geraniol possesses significant antioxidant activity that is attributed to direct antihemolytic effects protecting the membrane from free-radical-induced lipid peroxidation. Its action mechanism involves donating an allylic hydrogen atom from its terpene structure to neutralize peroxyl radicals, thus halting the chain reaction degrading membrane lipids [75]. High efficacy observed

in cinnamon · geranium and tea tree · geranium interactions, therefore, suggests a potent synergy, wherein geranium's MTPO stabilizes membrane structure, while compounds from other oils act via complementary mechanisms.

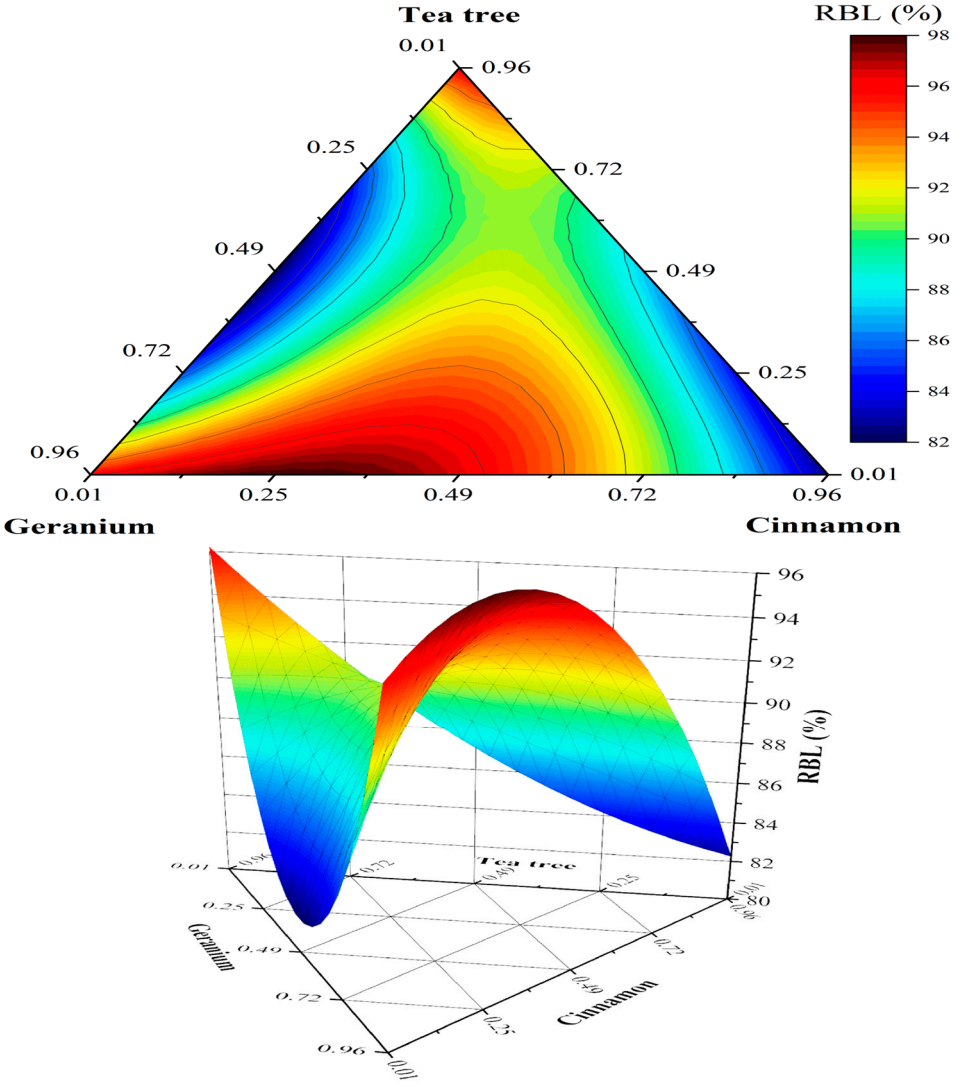



**Figure 5.** Ternary plot (**top**) and response surface (**bottom**) for red blood cell lysis inhibition (% inhibition) by the essential oil blend. Ginger proportion constant at 0.014.

Tea tree oil, also rich in MTPO (45.61%) but with a distinct profile dominated by terpinen-4-ol, was a major contributor to observed anti-hemolytic activity. Like geraniol, terpinen-4-ol is a monoterpene alcohol that alters membrane dynamics, increasing stability. Its action is associated with an ability to fill lipid bilayer voids, decreasing membrane fluidity and rendering it less susceptible to damage [76]. Terpinen-4-ol reportedly inhibits reactive oxygen species (ROS) production, a key hemolysis prevention mechanism, as erythrocytes are vulnerable to ROS attack due to high polyunsaturated fatty acid and hemoglobin concentrations [77]. Besides simple radical scavenging, terpinen-4-ol reportedly modulates inflammatory signaling pathways: for instance, by inhibiting tumor necrosis factor-alpha (TNF-α), which can promote oxidative stress and hemolysis [78]. Significant geranium oil interaction can therefore be explained by combined action from complementary MTPO profiles, wherein geraniol and citronellol provide structural stabilization, while terpinen-4-ol adds an antioxidant and anti-inflammatory protective layer.

Ginger oil, dominated by sesquiterpenes (SQTP) like α-zingiberene and β-sesquiphellandrene (constituting 71.07% total oil, Table 3), plays a crucial role through

synergistic action, particularly its highly significant synergistic interaction with cinnamon oil. Sesquiterpenes are larger, more lipophilic molecules than monoterpenes, allowing for deep partitioning into the membrane's hydrophobic core. They not only protect fatty acids from peroxidation but can also modulate integral membrane protein activity; compounds like α-zingiberene demonstrate potent free-radical scavenging activity [79]. Furthermore, sesquiterpenes can decrease membrane rigidity under certain conditions, enabling a cell to better withstand osmotic stress without rupturing [80]. Observed cinnamon synergy could be attributed to a mechanism where ginger sesquiterpenes protect the membrane interior and modulate physical properties, while cinnamon's components act on the membrane surface, creating a multilayered, multifunctional defense system.

Cinnamon oil, composed of 89.97% aromatic aldehydes (ALAR) (Table 3), with (E)-cinnamaldehyde as its major component, appears to have a more modulatory than directly protective role in this assay. Mixtures with highest pure cinnamon concentration, like mixture 7 (81.7% lysis inhibition), were not the most effective. High cinnamaldehyde concentrations alone are not optimal and could be membrane disruptive, due to high reactivity as an α,β-unsaturated aldehyde. Cinnamaldehyde can react with biological nucleophiles like membrane protein thiol groups and glutathione, a key endogenous antioxidant in erythrocytes [81]. Resulting glutathione depletion can render a cell vulnerable to oxidative damage, explaining why cinnamon oil alone is not highly protective. However, its capacity for a positive relationship with ginger and geranium is key. Observed synergy suggests that other antioxidant compounds from geranium and ginger, which may regenerate glutathione or protect thiol groups, can contribute to an overall protective effect. Terpenes from other oils, for example, could act as initial "shields," allowing cinnamaldehyde to exert other beneficial effects, like ion channel modulation, without causing toxicity.

Cinnamon oil's primary contribution was synergistic: a finding that contrasts with its low predicted individual efficacy (80.8 coefficient) and its reported pro-hemolytic potential. For instance, literature indicates that cinnamaldehyde can induce hemolysis exceeding 50% at 100 μg/mL [82]. The present study, however, reveals its role as a potent modulator, particularly with ginger and geranium—an effect not captured in isolated component analyses. A strong antagonistic connection between tea tree and geranium oils was a crucial finding, yielding the design's lowest inhibition (81.1%). This outcome is counterintuitive, as both oils individually demonstrated high efficacy (97.4 and 96.5 coefficients, respectively), a result consistent with literature attributing membrane-stabilizing effects to their principal monoterpene alcohols (terpinen-4-ol, citronellol). Published data confirm that tea tree oil can inhibit peroxide-induced lysis by over 60% [83], and geranium oil can provide over 70% protection in similar assays [17]. The observed antagonism thus challenges any assumption, based on a simple summation of individual effects. Ginger's most significant contribution was synergistic. While published studies report its moderate anti-hemolytic capacity, achieving ~45–55% inhibition at 0.5 mg/mL [30], its synergy with cinnamon in this study proved to be fundamental to obtaining over 95% protection. Ultimately, while literature validates the individual activity of each oil, these mixture-design results demonstrate that optimizing cytoprotection depends on a precise balance that leverages synergies while avoiding antagonisms.

Taken together, erythrocyte membrane protection is not attributable to a single essential oil or phytochemical group's action, but rather stems from complex, significant synergistic interactions established among them, a finding constituting a fundamental principle in scientific phytochemical product formulation. A combination of MTPO from geranium and tea tree, which intercalate to stabilize the lipid bilayer surface, with ginger's sesquiterpenes, which safeguard the hydrophobic core and modulate membrane's physical properties, emerges as the key mechanism achieving high lysis inhibition. Within this

system, cinnamon's cinnamaldehyde acts as a potent modulator whose contribution is beneficial only in a balanced mixture context, mitigating its potential cytotoxicity. Study findings demonstrate phytochemical synergy-based formulation superiority over individual component-based ones, providing crucial insight into developing new cytoprotective formulations with potential biomedical and cosmeceutical applications.

### *3.6. Catalase Activity*

Oxidative stress is a deleterious process resulting from an imbalance between reactive oxygen species (ROS) production and an organism's capacity to neutralize them via antioxidant defenses. Erythrocytes are particularly exposed to high oxidative stress, a consequence of their oxygen transport ability. Catalase (CAT), a crucial endogenous antioxidant enzyme, protects cells, including erythrocytes, against damage induced by hydrogen peroxide ($H_2O_2$), a major ROS, catalyzing its decomposition into water and oxygen. Investigating how natural compounds, like essential oils, can modulate this enzyme's activity is therefore of great interest for developing strategies to mitigate oxidative damage.

Catalase activity (CA), evaluated within the experimental design (Table 5), served as a key response variable determining essential oil mixtures' antioxidant potential. The results revealed a moderate CA variation, with values ranging from 112.65 to 160.86 kU/g Hb across 22 formulations. Mixtures inducing high enzymatic activity included mixture 7 (high in cinnamon), which achieved a maximum value of 160.86 KU/g Hb, followed by mixture 10 (cinnamon and tea tree) at 153.86 kU/g Hb. Mixtures 12 and 13 (combinations of ginger, cinnamon, and tea tree) also yielded high CA values of 152.77 and 145.38 kU/g Hb, respectively. Conversely, mixtures with lowest CA values were mixture 18 (tea tree and geranium) at 112.65 kU/g Hb and mixture 8 (ginger and geranium) at 117.92 kU/g Hb. These data preliminarily suggest cinnamon essential oil's presence, either alone or in combination, is a determining factor for enhanced catalase activity.

Analysis of variance (ANOVA), presented in Table 8, provided robust statistical validation for experimental observations. Overall model significance confirmed essential oil proportion variations predictably, and nonrandomly explained catalase activity. While a linear mixture term indicated that individual oils exert a significant CA effect, the most revealing aspect was high significance from multiple binary interactions. Ginger · tea tree ($x_1 \cdot x_3$) interaction was most influential, demonstrating strong interdependence between these two oils. Its high F value indicates that the variation explained by this relationship is 15 times greater than unexplained variation, underscoring its model importance. Similarly, significant interactions were confirmed for ginger · geranium ($x_1 \cdot x_4$), cinnamon · tea tree ($x_2 \cdot x_3$), cinnamon · geranium ($x_2 \cdot x_4$), and tea tree · geranium ($x_3 \cdot x_4$); these terms' significance provides fundamental evidence that oil effects are not merely additive. Instead, one oil's effect on catalase activity critically depends on another oil's concentration within the mixture, providing a statistical basis for synergy and antagonism phenomena discussed subsequently.

A predictive model (Equation (9)) was generated to quantify each component's influence on catalase activity (CA), exhibiting an $R^2$ of 97.06% and indicating a suitable fit with experimental data. Its linear coefficients show all oils make a positive contribution to catalase activity, with cinnamon having the highest coefficient, confirming its predominant role. Furthermore, positive coefficients for pairs like ginger · geranium and cinnamon · tea tree confirmed the ANOVA-observed synergies, whereby these oil combinations enhanced enzymatic activity beyond individual effects. In contrast, tea tree · geranium term had a negative coefficient of significant magnitude, suggesting a strong antagonistic effect. This antagonism is consistent with the low CA value observed in mixture 18, composed primarily of these two oils. Figure 6 graphically illustrates these competing effects; the ternary plot and response surface show that catalase activity increases significantly in

regions with high cinnamon concentrations, while combinations of geranium and tea tree (at the triangle's base) tend to decrease the response.

$$\begin{aligned} \text{CA (kU/g Hb)} = {} & 129.949 \cdot \textit{Ginger} + 163.023 \cdot \textit{Cinnamon} + 138.808 \cdot \textit{Tea Tree} \\ & + 139.032 \cdot \textit{Geranium} + 77.765 \cdot (\textit{Ginger} \cdot \textit{Tea Tree}) + 83.697 \cdot (\textit{Ginger} \cdot \textit{Geranium}) \\ & + 80.74 \cdot (\textit{Cinamon} \cdot \textit{Tea Tree}) - 62.25 \cdot (\textit{Cinamon} \cdot \textit{Geranium}) - 117.93 \cdot (\textit{Tea Tree} \cdot \textit{Geranium}) \end{aligned} \quad (9)$$

Cinnamon essential oil emerged as most influential factor, an effect attributed to its particular chemical composition. Aromatic aldehydes (ALAR) dominate the oil, constituting 89.97% total (Table 3), with major components being (E)-cinnamaldehyde (77.56%) and M-cinnamaldehyde (9.67%) (Table 2). Potent capacity from this oil to increase catalase activity is supported by scientific evidence. In vivo studies demonstrate that cinnamaldehyde can enhance antioxidant defenses, including increased erythrocyte catalase levels and activity. A proposed mechanism is activation of the nuclear factor erythroid 2 (Nrf2) pathway, a master regulator in expressing genes encoding antioxidant enzymes, including catalase [84]. Principal component action explains the high positive coefficient in Equation (9) and why mixture 7 (high in cinnamon, with 86.02% ALAR; Figure 3) exhibited maximum catalase activity (160.86 kU/g Hb).

Ginger essential oil, characterized by high sesquiterpene (SQTP) content (71.07%, Table 3) with α-zingiberene as principal component (33.77%, Table 2), also positively contributed to catalase activity. While the literature on direct effects from specific sesquiterpenes on erythrocyte catalase is limited, ginger extracts possess known potent antioxidant properties. These compounds can act as free-radical scavengers, reducing a cell's overall ROS load; decreasing available substrate ($H_2O_2$) reduces burden on the catalase enzyme, helping to preserve its structural integrity and catalytic activity [85]. However, ginger's most significant role identified here lies in its statistically significant synergistic interactions with tea tree ($x_1 \cdot x_3$) and geranium ($x_1 \cdot x_4$). This suggests that while its individual contribution is important, its presence enhances other oils' action. Mixture 21 (high in ginger, tea tree, and geranium), for example, showed high catalase activity (144.3 kU/g Hb) that was greater than expected from a simple individual effect summation, highlighting a complementary or synergistic mechanism.

Tea tree oil, with a balanced monoterpene (MTP, 44.95%) and oxygenated monoterpenoid (MTPO, 45.61%) composition, dominated by terpinen-4-ol (Tables 2 and 3), exhibited complex, dual functionality. Individually, the oil promoted catalase activity, indicated by its positive linear coefficient. The effect's mechanism involves terpinen-4-ol, a monoterpene alcohol, donating a hydrogen atom from its hydroxyl group to neutralize free radicals, while other components like γ-terpinene (21.17%) and α-terpinene (10.55%) also act as radical scavengers, due to conjugated diene systems [86]. However, the most relevant finding was tea tree oil's involvement in a negative, antagonistic geranium oil interaction ($x_3 \cdot x_4$). This antagonism manifested in mixture 18, which was composed almost exclusively from these two oils, presenting the lowest CA value (112.65 kU/g Hb). Results suggest that despite individual antioxidant properties, a specific combination of terpinen-4-ol with geranium's principal constituents (citronellol and geraniol) leads to a detrimental functional effect on the catalase enzyme. A biochemical mechanism underlying such antagonism likely involves interactions at the erythrocyte membrane level. Lipophilic terpenoids can insert themselves into the lipid bilayer. It is possible that a specific combination of monoterpenoids from tea tree and geranium may alter membrane fluidity, permeability, or structural integrity. A lipid microenvironment perturbation could then negatively affect the catalase enzyme's three-dimensional conformation or hinder its substrate ($H_2O_2$) access, thereby reducing its catalytic efficiency.

**Table 8.** Analysis of variance for the effect of evaluated essential oils on catalase activity (kU/g Hb).

| Source | Sum of Squares | df | Mean Square | F-Value | *p*-Value |
|---|---|---|---|---|---|
| Model | 2235.84 | 9 | 248.43 | 4.93 | 0.006 |
| Linear mixture | 955.47 | 3 | 318.49 | 6.32 | 0.008 |
| $x_1$*$x_2$ | 41.14 | 1 | 41.14 | 0.8165 | 0.660 |
| $x_1$*$x_3$ | 760.81 | 1 | 760.81 | 15.10 | 0.001 |
| $x_1$*$x_4$ | 3.96 | 1 | 3.96 | 0.0786 | 0.005 |
| $x_2$*$x_3$ | 170.38 | 1 | 170.38 | 3.38 | 0.002 |
| $x_2$*$x_4$ | 6.85 | 1 | 6.85 | 0.1358 | 0.017 |
| $x_3$*$x_4$ | 198.21 | 1 | 198.21 | 3.93 | 0.003 |
| Lack of fit | 540.73 | 8 | 67.59 | 4.23 | 0.090 |
| Total | 2840.56 | 21 | | | |

Geranium essential oil, rich in MTPO (77.32%) with citronellol and geraniol as principal constituents (Tables 2 and 3), similarly exhibited dual functionality. Its positive linear coefficient indicated an inherent benefit, but its dominant effect in certain combinations was its antagonistic effect with tea tree oil. An underlying mechanism for such antagonism may be multifactorial. One hypothesis is that certain terpenoids from these oils alter erythrocyte membrane fluidity and integrity. A resulting perturbation could indirectly affect the conformation or stability of membrane-associated or intracellular enzymes, such as catalase, reducing its catalytic efficiency. Another possibility is binding site competition or a direct molecular synergism between components, resulting in an inactive or less active complex. Low activity in mixture 8 (ginger and geranium) further points to unfavorable geranium interactions that do not have a potent activator like cinnamon.

Published research indicates that cinnamaldehyde, cinnamon's primary phytochemical, possesses direct antioxidant capacity and can upregulate antioxidant enzyme expression [84]. The maximum activity value found in a cinnamon-rich mixture (160.86 kU/g Hb) provides quantitative in vitro support in an erythrocyte system for this dual activity. Likewise, ginger oil's positive, albeit smaller, contribution aligns with in vivo studies reporting increased serum catalase in rats pre-treated with ginger extract, an effect attributed to compounds such as gingerol [27]. The analysis of mixture interactions, however, yields the most significant findings. A strong antagonism observed between tea tree and geranium oils, which resulted in the lowest catalase activity, represents a particularly critical finding. This outcome is unexpected, as published data indicate that geranium oil, through its component geraniol, generally increases catalase activity in mammalian tissues via activation of the Nrf2 pathway, a master regulator of the antioxidant response [87]. Conversely, research on tea tree oil's effect on mammalian catalase is notably scarce; some studies suggest its main component, terpinen-4-ol, may induce oxidative stress in certain cells, which could explain an enzymatic inhibition [83]. The antagonism identified in this study therefore suggests that combining terpinen-4-ol with geranium's monoterpenoids (citronellol and geraniol) in the erythrocyte membrane microenvironment leads to a functional inhibition of catalase—a result that is not predictable from single-oil studies.

Overall, cinnamon essential oil was most potent and determining agent in increasing catalase activity: an effect primarily attributed to its high (E)-cinnamaldehyde concentration. While other essential oils also contributed positively individually, their final effects were strongly conditioned by a complex relationship network. Observed synergies, particularly those involving ginger, suggest that combining different phytochemical classes may offer a multifaceted approach to enhancing antioxidant defenses. However, a critical finding, the strong antagonism between tea tree and geranium, underscores a fundamental principle: in essential oil mixture formulation, effects are not merely additive, as specific intercomponent interactions can lead to unexpected or counterproductive results.

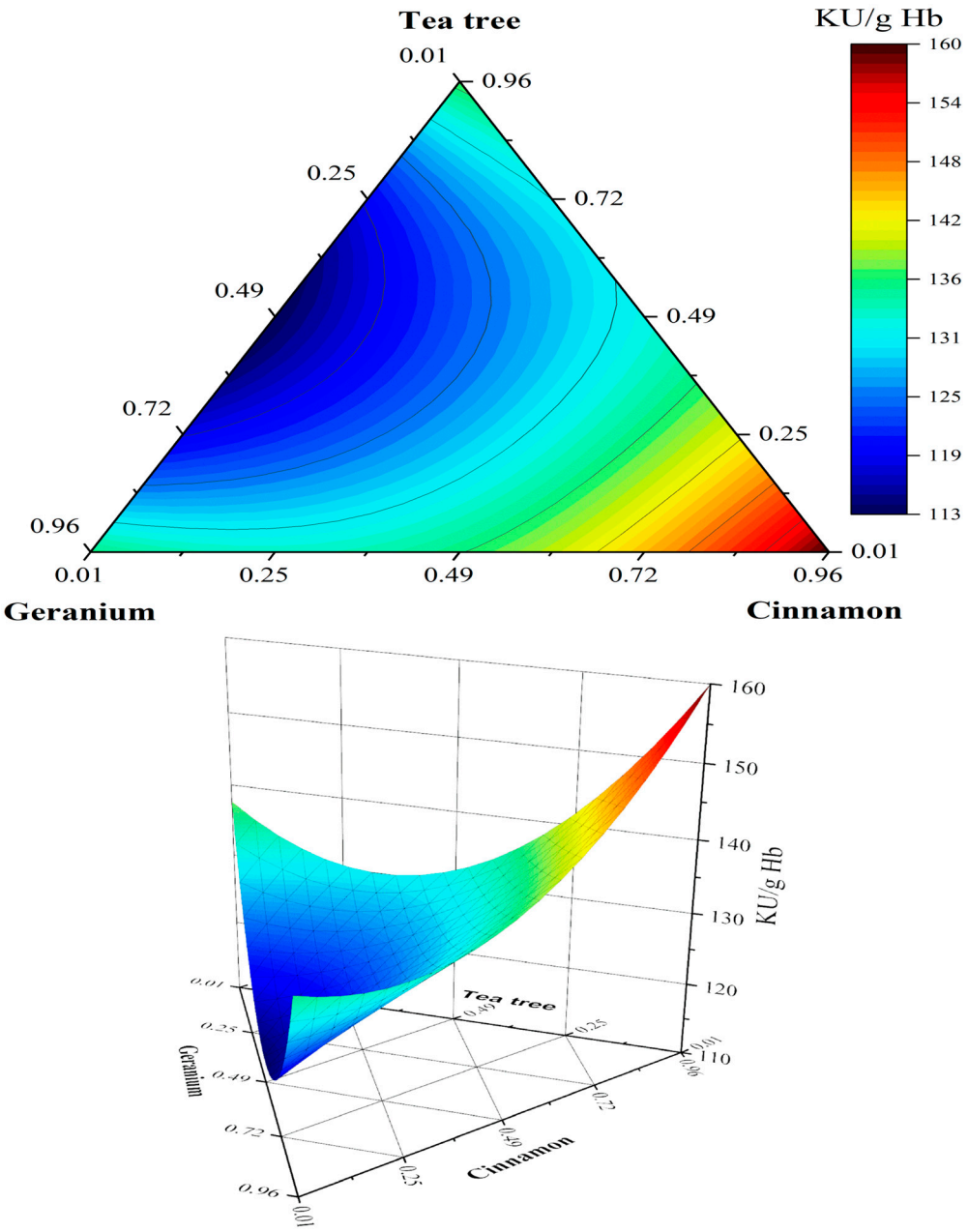



**Figure 6.** Catalase activity (kU/g Hb) as a function of essential oil blend composition: ternary plot (**top**) and response surface (**bottom**). Ginger proportion constant at 0.014.

### *3.7. Optimization and Validation*

Multiobjective optimization was performed to identify an ideal essential oil mixture for promoting cutaneous healing. Response variables were weighted on a one to five importance scale, including catalase activity (5), red blood cell lysis inhibition (5), and UV-B radiation absorption capacity (3). Optimization objective was to find a blend maximizing all three responses. Using Equation (4), this procedure identified an optimal mixture with the following essential oil proportions (fraction): ginger ($x_1$) 0.317, cinnamon ($x_2$) 0.391, tea tree ($x_3$) 0.145, and geranium ($x_4$) 0.147. Figure 7 details this optimization process graphically. An overlaid contour plot displays experimental space for essential oil components, with the optimal mixture located at a response contour intersection.

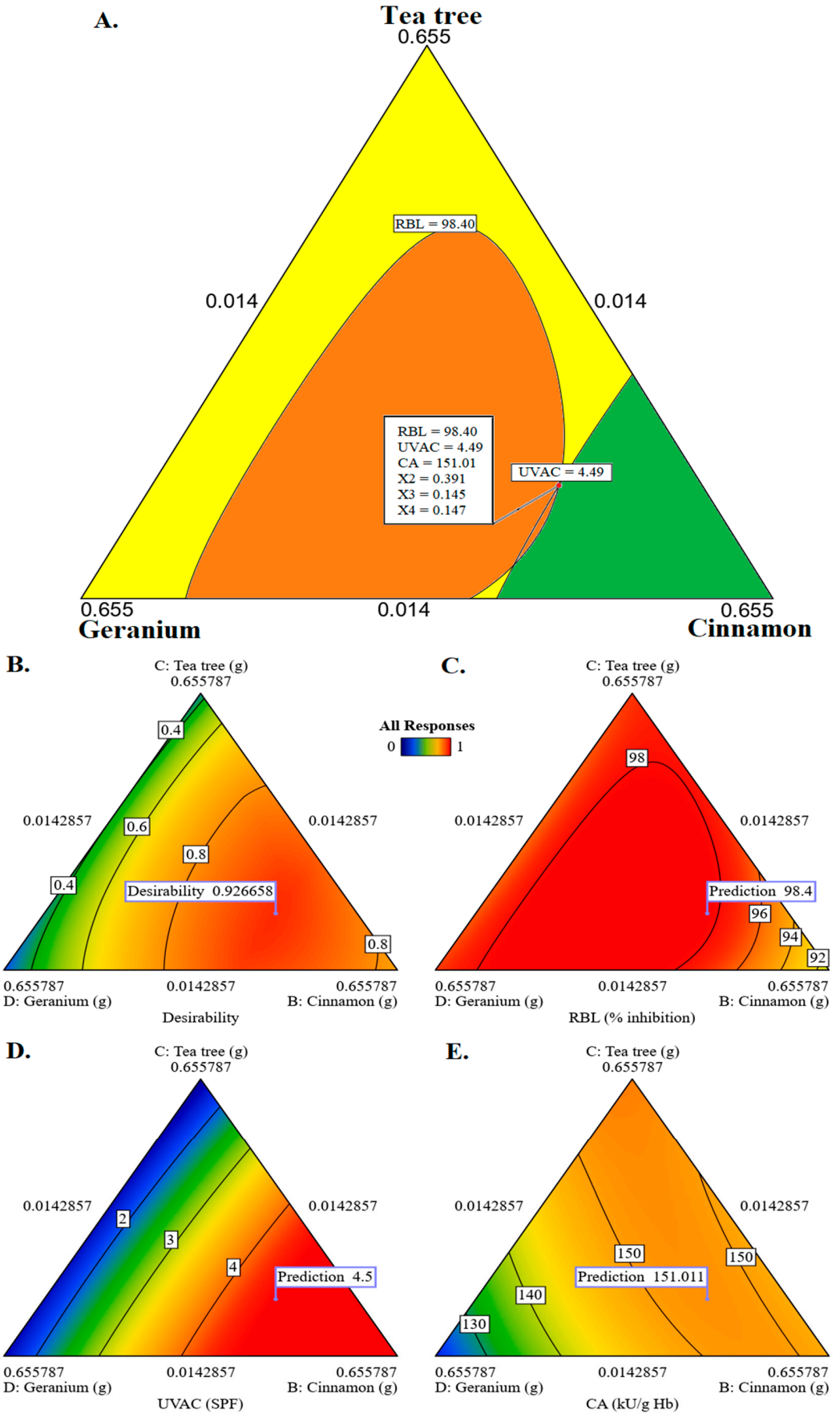



**Figure 7.** Contour plots from the mixture design. (**A**) Overlay plot for simultaneous optimization; (**B**) Desirability function; and individual response surfaces for (**C**) RBL (% inhibition), (**D**) UVAC (SPF), and (**E**) CA (kU/g Hb). Ginger proportion constant at 0.317.

Resulting formulation represents the specific combination that maximizes balance among the three studied responses (CA, UVAC, and RBL), achieving a maximum desirability value $D(x) = 0.927$. Its position at the design space edge reveals that optimization was constrained by high response threshold values. Accompanying ternary graphs show the predicted values for responses in this formulation, with two (RBL and UVAC) coinciding with maximum established criteria limits.

Finally, optimization model was experimentally validated by preparing and evaluating the optimal essential oil formulation. Experimental results for the three response variables were compared with the values predicted from developed models (Equations (7)–(9)). Data in Table 9 demonstrate high concordance between predictions and experimental results. Obtained *p*-values for UV-B absorption capacity (UVAC), erythrocyte lysis inhibition (RBL), and catalase activity (CA) were 0.086, 0.293, and 0.666, respectively. In all three cases, *p*-values were greater than significance level ($\alpha = 0.05$), indicating no significant differences between observed and predicted mean values (Table 9). Low variation coefficients, consistently under 3%, support measurement reliability. Validation results confirm that the desirability function approach is an effective methodology for rational multicomponent essential oil mixture design. This approach allows for a reliable prediction of their synergistic and multifunctional bioactivity.

**Table 9.** Predicted versus experimental values for the optimal essential oil mixture.

| Responses | Units | Predicted | Experimental ($n = 3$) | | | | | |
|---|---|---|---|---|---|---|---|---|
| | | | Mean | Standard Deviation | Coefficient of Variation | Min | Max | *p*-Value |
| UVAC | SPF | 4.49 | 4.51 | 0.058 | 1.280 | 4.51 | 4.62 | 0.086 |
| RBL | % Inhibition | 98.40 | 100.08 | 2.683 | 2.681 | 97.04 | 102.12 | 0.293 |
| AC | kU/g Hb | 151.01 | 151.19 | 1.990 | 1.316 | 149.21 | 153.19 | 0.666 |

## 4. Conclusions

The primary objective of this study—to develop an optimized active ingredient from a mixture of ginger, cinnamon, tea tree, and geranium essential oils using a "formulation by design" approach—was successfully achieved. Initial characterization confirmed each oil's distinct phytochemical profile and underscored the need for a balanced formulation to mitigate the cytotoxicity observed in the pure components. Results demonstrated that mixture bioactivity is a function of complex, nonadditive interactions, rather than simple component summation. Dose–response data from essential oils tested against skin fibroblasts revealed a clear cytotoxic hierarchy: cinnamon > ginger > tea tree> geranium. High photoprotective capacity was attributed primarily to cinnamon oil's direct effect and aromatic aldehydes. In contrast, erythrocyte membrane stabilization emerged from a complex synergy between MTPO from geranium and tea tree oils and sesquiterpenes from ginger. Catalase activity modulation also depended on cinnamon's components; this nonadditive behavior was further confirmed by the notable antagonism identified between tea tree and geranium oils. Multiobjective optimization via a desirability function yielded the following final formulation: 31.7% ginger, 39.1% cinnamon, 14.5% tea tree, and 14.7% geranium. Optimal mixture validation confirms the predictive reliability from developed statistical models. This work provides a rationally designed blend with promising multifunctional bioactivities. However, as a foundational study, its limitations must be acknowledged. The logical and necessary next steps are to advance the evaluation of this optimized blend into more direct models of skin healing. Future work will involve in vitro studies, such as fibroblast migration (scratch assays) and proliferation assays, to directly assess its effects on

key cellular healing processes. Subsequently, in vivo studies will be warranted to evaluate the definitive skin-healing efficacy and safety profile of the final formulated product.

**Author Contributions:** A.Z.B.; Writing—original draft, Methodology, Data curation, Conceptualization, and Investigation. A.P.D.; Writing—original draft, Investigation, Formal analysis, Data curation, and Conceptualization. F.F.L.; Writing—review and editing, Writing—original draft, Formal analysis, Data curation, Supervision, and Investigation. All authors have read and agreed to the published version of the manuscript.

**Funding:** This research and APC was funded by the University of Antioquia (Colombia), Committee for Research Development (CODI, Grant No. 2017-15667-ES84170157—Engineering and Technology Area).

**Institutional Review Board Statement:** Not applicable.

**Informed Consent Statement:** Not applicable.

**Data Availability Statement:** The original contributions presented in this study are included in the article. Further inquiries can be directed to the corresponding author.

**Conflicts of Interest:** Author Adriana Pulido Diaz was employed by the company Agrosavia C.I La Selva. The remaining authors declare that the research was conducted in the absence of any commercial or financial relationships that could be construed as a potential.

## References

1. Yadav, N.; Saini, N.; Rathi, N.; Chauhan, S.; Sharma, P.K.; Sangwan, N.S. Health-promoting effects of cinnamon. In *Cinnamon*; Ramadan, M.F., Farag, M.A., Eds.; Academic Press: Cambridge, MA, USA, 2025; pp. 219–241.
2. Cardoso-Ugarte, G.; López-Malo, A.; Sosa-Morales, M. Cinnamon (Cinnamomum zeylanicum) Essential Oils. *Essent. Oils Food Preserv. Flavor Saf.* **2016**, 339–347. [CrossRef]
3. Tamer, C.E.; Özkan Karabacak, A.; Durgut Malçok, S. Drinks and foods enriched with cinnamon. In *Cinnamon*; Ramadan, M.F., Farag, M.A., Eds.; Academic Press: Cambridge, MA, USA, 2025; pp. 557–582.
4. Funk, J.L.; Frye, J.B.; Oyarzo, J.N.; Chen, J.; Zhang, H.; Timmermann, B.N. Anti-Inflammatory Effects of the Essential Oils of Ginger (*Zingiber officinale* Roscoe) in Experimental Rheumatoid Arthritis. *PharmaNutrition* **2016**, *4*, 123–131. [CrossRef]
5. Uddin, J.; Ahmed, H.; Asiri, Y.I.; Kamal, G.M.; Musharraf, S.G. Ginger essential oil: Chemical composition, extraction, characterization, pharmacological activities, and applications. In *Essential Oils*; Nayik, G.A., Ansari, M.J., Eds.; Academic Press: Cambridge, MA, USA, 2023; pp. 345–376.
6. Olsson, M.; Jarbrink, K.; Divakar, U.; Bajpai, R.; Upton, Z.; Schmidtchen, A.; Car, J. The humanistic and economic burden of chronic wounds: A systematic review. *Wound Repair. Regen.* **2019**, *27*, 114–125. [CrossRef] [PubMed]
7. Sharifi-Rad, J.; Sureda, A.; Tenore, G.C.; Daglia, M.; Sharifi-Rad, M.; Valussi, M.; Tundis, R.; Sharifi-Rad, M.; Loizzo, M.R.; Ademiluyi, A.O.; et al. Biological Activities of Essential Oils: From Plant Chemoecology to Traditional Healing Systems. *Molecules* **2017**, *22*, 70. [CrossRef]
8. Mssillou, I.; Amrati, F.E.; Saghrouchni, H.; El Abdali, Y.; Lefrioui, Y.; Batiha, G.E.; Giesy, J.P.; Aboul-Soud, M.A.M.; Hassani, R.; Khalid, A.; et al. Recent advances in the use of essential oils and their nanoformulations for wound treatment. *Burns* **2025**, *51*, 107260. [CrossRef] [PubMed]
9. Lv, C.; Yuan, X.; Zeng, H.W.; Liu, R.H.; Zhang, W.D. Protective effect of cinnamaldehyde against glutamate-induced oxidative stress and apoptosis in PC12 cells. *Eur. J. Pharmacol.* **2017**, *815*, 487–494. [CrossRef]
10. Minozzo, M.; de Souza, M.A.; Bernardi, J.L.; Puton, B.M.S.; Valduga, E.; Steffens, C.; Paroul, N.; Cansian, R.L. Antifungal activity and aroma persistence of free and encapsulated Cinnamomum cassia essential oil in maize. *Int. J. Food Microbiol.* **2023**, *394*, 110178. [CrossRef]
11. Gu, K.; Feng, S.; Zhang, X.; Peng, Y.; Sun, P.; Liu, W.; Wu, Y.; Yu, Y.; Liu, X.; Liu, X.; et al. Deciphering the antifungal mechanism and functional components of cinnamomum cassia essential oil against Candida albicans through integration of network-based metabolomics and pharmacology, the greedy algorithm, and molecular docking. *J. Ethnopharmacol.* **2024**, *319*, 117156. [CrossRef] [PubMed]
12. Paiano, R.B.; de Sousa, R.L.M.; Bonilla, J.; Moreno, L.Z.; de Souza, E.D.F.; Baruselli, P.S.; Moreno, A.M. In vitro effects of cinnamon, oregano, and thyme essential oils against Escherichia coli and Trueperella pyogenes isolated from dairy cows with clinical endometritis. *Theriogenology* **2023**, *196*, 106–111. [CrossRef]

13. Farahpour, M.R.; Habibi, M. Evaluation of the wound healing activity of an ethanolic extract of Ceylon cinnamon in mice. *Veterinární Medicína* **2012**, *57*, 53–57. [CrossRef]
14. Yuan, X.; Han, L.; Fu, P.; Zeng, H.; Lv, C.; Chang, W.; Runyon, R.S.; Ishii, M.; Han, L.; Liu, K.; et al. Cinnamaldehyde accelerates wound healing by promoting angiogenesis via up-regulation of PI3K and MAPK signaling pathways. *Lab. Investig.* **2018**, *98*, 783–798. [CrossRef] [PubMed]
15. Upadhyay, R.; Lothe, N.B.; Bawitlung, L.; Singh, S.; Singh, M.K.; Kumar, P.; Verma, R.K.; Tandon, S.; Pal, A.; Verma, R.S. Secondary metabolic profile of rose-scented geranium: A tool for characterization, distinction and quality control of Indian genotypes. *Ind. Crops Prod.* **2022**, *187*, 115487. [CrossRef]
16. El Aanachi, S.; Gali, L.; Nacer, S.N.; Bensouici, C.; Dari, K.; Aassila, H. Phenolic contents and in vitro investigation of the antioxidant, enzyme inhibitory, photoprotective, and antimicrobial effects of the organic extracts of *Pelargonium graveolens* growing in Morocco. *Biocatal. Agric. Biotechnol.* **2020**, *29*, 101819. [CrossRef]
17. Boukhatem, M.N.; Sudha, T.; Darwish, N.H.E.; Nada, H.G.; Mousa, S.A. Rose-scented geranium essential oil from Algeria (*Pelargonium graveolens* L'Herit.): Assessment of antioxidant, anti-inflammatory and anticancer properties against different metastatic cancer cell lines. *Ann. Pharm. Fr.* **2022**, *80*, 383–396. [CrossRef]
18. Pereira, R.B.; Rahali, F.Z.; Nehme, R.; Falleh, H.; Jemaa, M.B.; Sellami, I.H.; Ksouri, R.; Bouhallab, S.; Ceciliani, F.; Abdennebi-Najar, L.; et al. Anti-inflammatory activity of essential oils from Tunisian aromatic and medicinal plants and their major constituents in THP-1 macrophages. *Food Res. Int.* **2023**, *167*, 112678. [CrossRef]
19. Naeini, A.R.; Nazeri, M.; Shokri, H. Antifungal activity of *Zataria multiflora*, *Pelargonium graveolens* and *Cuminum cyminum* essential oils towards three species of Malassezia isolated from patients with pityriasis versicolor. *J. De Mycol. Médicale* **2011**, *21*, 87–91. [CrossRef]
20. Androutsopoulou, C.; Christopoulou, S.D.; Hahalis, P.; Kotsalou, C.; Lamari, F.N.; Vantarakis, A. Evaluation of Essential Oils and Extracts of Rose Geranium and Rose Petals as Natural Preservatives in Terms of Toxicity, Antimicrobial, and Antiviral Activity. *Pathogens* **2021**, *10*, 494. [CrossRef]
21. Edwards-Jones, V.; Buck, R.; Shawcross, S.G.; Dawson, M.M.; Dunn, K. The effect of essential oils on methicillin-resistant Staphylococcus aureus using a dressing model. *Burns* **2004**, *30*, 772–777. [CrossRef]
22. Battisti, M.A.; Caon, T.; Machado de Campos, A. A short review on the antimicrobial micro- and nanoparticles loaded with *Melaleuca alternifolia* essential oil. *J. Drug Deliv. Sci. Technol.* **2021**, *63*, 102283. [CrossRef]
23. Garozzo, A.; Timpanaro, R.; Stivala, A.; Bisignano, G.; Castro, A. Activity of *Melaleuca alternifolia* (tea tree) oil on Influenza virus A/PR/8: Study on the mechanism of action. *Antivir. Res.* **2011**, *89*, 83–88. [CrossRef]
24. Low, P.; Clark, A.M.; Chou, T.C.; Chang, T.C.; Reynolds, M.; Ralph, S.J. Immunomodulatory activity of *Melaleuca alternifolia* concentrate (MAC): Inhibition of LPS-induced NF-kappaB activation and cytokine production in myeloid cell lines. *Int. Immunopharmacol.* **2015**, *26*, 257–264. [CrossRef] [PubMed]
25. Ramadan, M.A.; Shawkey, A.E.; Rabeh, M.A.; Abdellatif, A.O. Promising antimicrobial activities of oil and silver nanoparticles obtained from *Melaleuca alternifolia* leaves against selected skin-infecting pathogens. *J. Herbal. Med.* **2020**, *20*, 100289. [CrossRef]
26. Hammer, K.A.; Carson, C.F.; Riley, T.V. Effects of *Melaleuca alternifolia* (tea tree) essential oil and the major monoterpene component terpinen-4-ol on the development of single- and multistep antibiotic resistance and antimicrobial susceptibility. *Antimicrob. Agents Chemother.* **2012**, *56*, 909–915. [CrossRef]
27. Yeh, H.-y.; Chuang, C.-h.; Chen, H.-c.; Wan, C.-j.; Chen, T.-l.; Lin, L.-y. Bioactive components analysis of two various gingers (*Zingiber officinale* Roscoe) and antioxidant effect of ginger extracts. *LWT—Food Sci. Technol.* **2014**, *55*, 329–334. [CrossRef]
28. Zhong, W.; Zhu, J.; Yi, J.; Zhao, C.; Shi, Y.; Kang, Q.; Huang, J.; Hao, L.; Lu, J. Biochemical analysis reveals the systematic response of motion sickness mice to ginger (*Zingiber officinale*) extract's amelioration effect. *J. Ethnopharmacol.* **2022**, *290*, 115077. [CrossRef]
29. Thongson, C.; Davidson, P.M.; Mahakarnchanakul, W.; Vibulsresth, P. Antimicrobial effect of Thai spices against Listeria monocytogenes and Salmonella typhimurium DT104. *J. Food Prot.* **2005**, *68*, 2054–2058. [CrossRef]
30. Abolaji, A.O.; Ojo, M.; Afolabi, T.T.; Arowoogun, M.D.; Nwawolor, D.; Farombi, E.O. Protective properties of 6-gingerol-rich fraction from *Zingiber officinale* (Ginger) on chlorpyrifos-induced oxidative damage and inflammation in the brain, ovary and uterus of rats. *Chem. Biol. Interact.* **2017**, *270*, 15–23. [CrossRef]
31. Al-Samydai, A.; Qaraleh, M.A.; Alshaer, W.; Al-Halaseh, L.K.; Issa, R.; Alshaikh, F.; Abu-Rumman, A.; Al-Ali, H.; Al-Dujaili, E.A.S. Preparation, Characterization, Wound Healing, and Cytotoxicity Assay of PEGylated Nanophytosomes Loaded with 6-Gingerol. *Nutrients* **2022**, *14*, 5170. [CrossRef] [PubMed]
32. Robledo Restrepo, S.M.; Quintero, J.; Higuita, J.; Fernández, M.; Murillo, J.; Restrepo, A.; Arbeláez, N.; Montoya, A.; Ospina, V.; Pineda, T.; et al. Caesalpinia spinosa (Molina) Kuntze: Una nueva promesa para el tratamiento tópico de la leishmaniasis cutánea. *Rev. De La Acad. Colomb. De Cienc. Exactas Físicas Y Nat.* **2020**, *44*, 915–936. [CrossRef]
33. Benkhaira, N.; Zouine, N.; Fadil, M.; Ibnsouda Koraichi, S.; El Hachlafi, N.; Jeddi, M.; Lachkar, M.; Fikri-Benbrahim, K. Application of mixture design for the optimum antibacterial action of chemically-analyzed essential oils and investigation of the antiadhesion ability of their optimal mixtures on 3D printing material. *Bioprinting* **2023**, *34*, e00299. [CrossRef]

34. Oyeleke, S.A.; Ajayi, A.M.; Umukoro, S.; Aderibigbe, A.O.; Ademowo, O.G. Anti-inflammatory activity of *Theobroma cacao* L. stem bark ethanol extract and its fractions in experimental models. *J. Ethnopharmacol.* **2018**, *222*, 239–248. [CrossRef]
35. Dutra, E.A.; Oliveira, D.A.G.d.C.; Kedor-Hackmann, E.R.M.; Santoro, M.I.R.M. Determination of sun protection factor (SPF) of sunscreens by ultraviolet spectrophotometry. *Rev. Bras. De Ciências Farm.* **2004**, *40*, 381–385. [CrossRef]
36. Weydert, C.J.; Cullen, J.J. Measurement of superoxide dismutase, catalase and glutathione peroxidase in cultured cells and tissue. *Nat. Protoc.* **2010**, *5*, 51–66. [CrossRef]
37. Amdoun, R.; Khelifi, L.; Khelifi-Slaoui, M.; Amroune, S.; Asch, M.; Assaf-Ducrocq, C.; Gontier, E. The Desirability Optimization Methodology; a Tool to Predict Two Antagonist Responses in Biotechnological Systems: Case of Biomass Growth and Hyoscyamine Content in Elicited Datura starmonium Hairy Roots. *Iran. J. Biotechnol.* **2018**, *16*, e1339. [CrossRef]
38. *ISO 3216:1997*; Oil of Cassia, Chinese Type (*Cinnamomum aromaticum* Nees, Syn. *Cinnamomum cassia* Nees Ex Blume). International Organization for Standardization: Geneva, Switzerland, 1997.
39. Denkova-Kostova, R.; Teneva, D.; Tomova, T.; Goranov, B.; Denkova, Z.; Shopska, V.; Slavchev, A.; Hristova-Ivanova, Y. Chemical composition, antioxidant and antimicrobial activity of essential oils from tangerine (*Citrus reticulata* L.), grapefruit (*Citrus paradisi* L.), lemon (*Citrus lemon* L.) and cinnamon (*Cinnamomum zeylanicum* Blume). *Z. Naturforsch C J. Biosci.* **2021**, *76*, 175–185. [CrossRef]
40. *ISO 4731:2012*; Essential oil of geranium (*Pelargonium x* ssp.). International Organization for Standardization: Geneva, Switzerland, 2012.
41. Pavan, B.; Dalpiaz, A.; Marani, L.; Beggiato, S.; Ferraro, L.; Canistro, D.; Paolini, M.; Vivarelli, F.; Valerii, M.C.; Comparone, A.; et al. Geraniol Pharmacokinetics, Bioavailability and Its Multiple Effects on the Liver Antioxidant and Xenobiotic-Metabolizing Enzymes. *Front. Pharmacol.* **2018**, *9*, 18. [CrossRef]
42. Salgado, F. El jengibre (*Zingiber officinale*). *Rev. Int. De Acupunt.* **2011**, *5*, 167–173. [CrossRef]
43. *ISO 16928:2014*; Essential Oil of Ginger (*Zingiber officinale* Roscoe). International Organization for Standardization: Geneva, Switzerland, 2014.
44. Carson, C.F.; Hammer, K.A.; Riley, T.V. Melaleuca alternifolia (Tea Tree) oil: A review of antimicrobial and other medicinal properties. *Clin. Microbiol. Rev.* **2006**, *19*, 50–62. [CrossRef]
45. Souza, C.F.; Baldissera, M.D.; Silva, L.d.L.; Geihs, M.A.; Baldisserotto, B. Is monoterpene terpinen-4-ol the compound responsible for the anesthetic and antioxidant activity of Melaleuca alternifolia essential oil (tea tree oil) in silver catfish? *Aquaculture* **2018**, *486*, 217–223. [CrossRef]
46. *ISO 4730:2025*; Essential oil of Melaleuca, terpinen-4-ol type (Tea Tree Oil). International Organization for Standardization: Geneva, Switzerland, 2025.
47. Badr, M.M.; Badawy, M.E.I.; Taktak, N.E.M. Characterization, antimicrobial activity, and antioxidant activity of the nanoemulsions of Lavandula spica essential oil and its main monoterpenes. *J. Drug Deliv. Sci. Technol.* **2021**, *65*, 102732. [CrossRef]
48. Neerman, M. Sesquiterpene lactones: A diverse class of compounds found in essential oils possessing antibacterial and antifungal properties. *Int. J. Aromather.* **2003**, *13*, 114–120. [CrossRef]
49. Jin, J.H.; Lee, D.U.; Kim, Y.S.; Kim, H.P. Anti-allergic activity of sesquiterpenes from the rhizomes of Cyperus rotundus. *Arch. Pharm. Res.* **2011**, *34*, 223–228. [CrossRef] [PubMed]
50. Narnoliya, L.K.; Jadaun, J.S.; Singh, S.P. The Phytochemical Composition, Biological Effects and Biotechnological Approaches to the Production of High-Value Essential Oil from Geranium. In *Essential Oil Research*; Malik, S., Ed.; Springer International Publishing: Cham, Switerland, 2019; pp. 327–352.
51. Xing, J.; Yang, C.; Zhang, L. Characterization of key flavor compounds in cinnamon bark oil extracts using principal component analysis. *Food Res. Int.* **2025**, *200*, 115446. [CrossRef]
52. Carrasco, A.; Martinez-Gutierrez, R.; Tomas, V.; Tudela, J. Lavandin (Lavandula x intermedia Emeric ex Loiseleur) essential oil from Spain: Determination of aromatic profile by gas chromatography-mass spectrometry, antioxidant and lipoxygenase inhibitory bioactivities. *Nat. Prod. Res.* **2016**, *30*, 1123–1130. [CrossRef]
53. Wanakhachornkrai, O.; Banglao, W.; Thongmee, A.; Sukplang, P. Determination of Antioxidant, Anti-Aging and Cytotoxicity Activity of the Essential Oils from Cinnamomum Zeylanicum. *J. Microbiol. Biotechnol. Food Sci.* **2020**, *10*, 436–440. [CrossRef]
54. Chang, W.L.; Cheng, F.C.; Wang, S.P.; Chou, S.T.; Shih, Y. Cinnamomum cassia essential oil and its major constituent cinnamaldehyde induced cell cycle arrest and apoptosis in human oral squamous cell carcinoma HSC-3 cells. *Environ. Toxicol.* **2017**, *32*, 456–468. [CrossRef]
55. Kairey, L.; Agnew, T.; Bowles, E.J.; Barkla, B.J.; Wardle, J.; Lauche, R. Efficacy and safety of Melaleuca alternifolia (tea tree) oil for human health-A systematic review of randomized controlled trials. *Front. Pharmacol.* **2023**, *14*, 1116077. [CrossRef]
56. Terzi, V.; Morcia, C.; Faccioli, P.; Vale, G.; Tacconi, G.; Malnati, M. In vitro antifungal activity of the tea tree (*Melaleuca alternifolia*) essential oil and its major components against plant pathogens. *Lett. Appl. Microbiol.* **2007**, *44*, 613–618. [CrossRef]
57. Kalhoro, M.T.; Zhang, H.; Kalhoro, G.M.; Wang, F.; Chen, T.; Faqir, Y.; Nabi, F. Fungicidal properties of ginger (*Zingiber officinale*) essential oils against Phytophthora colocasiae. *Sci. Rep.* **2022**, *12*, 2191. [CrossRef] [PubMed]

58. Shirooye, P.; Mokaberinejad, R.; Ara, L.; Hamzeloo-Moghadam, M. Volatile Constituents of Ginger Oil Prepared According to Iranian Traditional Medicine and Conventional Method: A Comparative Study. *Afr. J. Tradit. Complement. Altern. Med.* **2016**, *13*, 68–73. [CrossRef] [PubMed]
59. Hoferl, M.; Stoilova, I.; Wanner, J.; Schmidt, E.; Jirovetz, L.; Trifonova, D.; Stanchev, V.; Krastanov, A. Composition and Comprehensive Antioxidant Activity of Ginger (*Zingiber officinale*) Essential Oil from Ecuador. *Nat. Prod. Commun.* **2015**, *10*, 1085–1090. [CrossRef] [PubMed]
60. Fayoumi, L.; Khalil, M.; Ghareeb, D.; Chokr, A.; Bouaziz, M.; El-Dakdouki, M.H. Phytochemical constituents and therapeutic effects of the essential oil of rose geranium (*Pelargonium hybrid*) cultivated in Lebanon. *South. Afr. J. Bot.* **2022**, *147*, 894–902. [CrossRef]
61. *ISO 10993-5:2009*; Biological Evaluation of Medical Devices Part 5: Tests for In Vitro Cytotoxicity. International Organization for Standardization: Geneva, Switzerland, 2009.
62. Wei, L.; Yang, H.; Li, H.; Zhu, M.; Mi, S.; Lu, Q.; Liu, M.; Zu, Y. Comparison of chemical composition and activities of essential oils from fresh leaves of Pelargonium graveolens L′Herit. extracted by hydrodistillation and enzymatic pretreatment combined with a solvent-free microwave extraction method. *Ind. Crops Prod.* **2022**, *186*, 115204. [CrossRef]
63. Pontes, E.R.; de Souza Guedes, L.; da Silva, T.F.; Barbosa, F.C.B.; de Souza, B.W.S.; de Freitas Rosa, M.; Vieira, R.S.; Andrade, F.K. Development of silanized bacterial cellulose aerogels for the incorporation of natural oils with healing properties: Copaiba (*Copaifera officinalis*), bourbon geranium (*Pelargonium* X ssp.) essential oils and buriti (*Mauritia flexuosa*) vegetable oil. *Int. J. Biol. Macromol.* **2024**, *269*, 132266. [CrossRef]
64. Marionnet, C.; Nouveau, S.; Hourblin, V.; Pillai, K.; Manco, M.; Bastien, P.; Tran, C.; Tricaud, C.; de Lacharrière, O.; Bernerd, F. UVA1-Induced Skin Darkening Is Associated with Molecular Changes Even in Highly Pigmented Skin Individuals. *J. Investig. Dermatol.* **2017**, *137*, 1184–1187. [CrossRef]
65. Rittie, L.; Fisher, G.J. UV-light-induced signal cascades and skin aging. *Ageing Res. Rev.* **2002**, *1*, 705–720. [CrossRef] [PubMed]
66. Pavia, D.L.; Lampman, G.M.; Kriz, G.S.; Vyvyan, J.A. *Introduction to Spectroscopy*, 5th ed.; Cengage Learning: Boston, MA, USA, 2014.
67. Serpone, N.; Salinaro, A.; Emeline, A.V.; Horikoshi, S.; Hidaka, H.; Zhao, J. An in vitro systematic spectroscopic examination of the photostabilities of a random set of commercial sunscreen lotions and their chemical UVB/UVA active agents. *Photochem. Photobiol. Sci.* **2002**, *1*, 970–981. [CrossRef]
68. Silverstein, R.M.; Webster, F.X.; Kiemle, D. *Spectrometric Identification of Organic Compounds*, 7th ed.; Wiley: Hoboken, NJ, USA, 2005.
69. Priani, S.E. Formulation and Characterization Sunscreen Emulgel Containing Cinnamon Bark Oil (Cinnamomum Burmannii Nees Ex Blume). *Indones. J. Pharm. Sci. Technol.* **2025**, *12*, 85–92. [CrossRef]
70. Vella, F.M.; Cautela, D.; Laratta, B. Determination of Antioxidant Activity and Sun Protection Factor of Commercial Essential Oils. *Biol. Life Sci. Forum* **2021**, *6*, 96. [CrossRef]
71. Lohani, A.; Mishra, A.K.; Verma, A. Cosmeceutical potential of geranium and calendula essential oil: Determination of antioxidant activity and in vitro sun protection factor. *J. Cosmet. Dermatol.* **2019**, *18*, 550–557. [CrossRef]
72. Suva, M. Evaluation of Sun Protection Factor of *Zingiber officinale* Roscoe Extract by Ultraviolet Spectroscopy Method. *J. PharmaSciTech* **2014**, *3*, 95–97.
73. Masyita, A.; Mustika Sari, R.; Dwi Astuti, A.; Yasir, B.; Rahma Rumata, N.; Emran, T.B.; Nainu, F.; Simal-Gandara, J. Terpenes and terpenoids as main bioactive compounds of essential oils, their roles in human health and potential application as natural food preservatives. *Food Chem. X* **2022**, *13*, 100217. [CrossRef]
74. Cristani, M.; D'Arrigo, M.; Mandalari, G.; Castelli, F.; Sarpietro, M.G.; Micieli, D.; Venuti, V.; Bisignano, G.; Saija, A.; Trombetta, D. Interaction of four monoterpenes contained in essential oils with model membranes: Implications for their antibacterial activity. *J. Agric. Food Chem.* **2007**, *55*, 6300–6308. [CrossRef] [PubMed]
75. Singh, S.; Fatima, Z.; Ahmad, K.; Hameed, S. Fungicidal action of geraniol against Candida albicans is potentiated by abrogated CaCdr1p drug efflux and fluconazole synergism. *PLoS ONE* **2018**, *13*, e0203079. [CrossRef]
76. Liu, Y.; Tang, X.; Zhang, H.; Zheng, L.; Lai, P.; Guo, C.; Ma, J.; Chen, H.; Qiu, L. Terpinen-4-ol Improves Lipopolysaccharide-Induced Macrophage Inflammation by Regulating Glutamine Metabolism. *Foods* **2024**, *13*, 1842. [CrossRef]
77. Sivilotti, M.L. Oxidant stress and haemolysis of the human erythrocyte. *Toxicol. Rev.* **2004**, *23*, 169–188. [CrossRef]
78. Hart, P.H.; Brand, C.; Carson, C.F.; Riley, T.V.; Prager, R.H.; Finlay-Jones, J.J. Terpinen-4-ol, the main component of the essential oil of Melaleuca alternifolia (tea tree oil), suppresses inflammatory mediator production by activated human monocytes. *Inflamm. Res.* **2000**, *49*, 619–626. [CrossRef]
79. Karimian, M.; Riasi, A.; Ghasemi, E.; Mahyari, S.A. Effect of omega fatty acids sources alone or combined with essential oils on feed intake, apparent digestibility, rumen microbiome and blood metabolites during peripartum period of ewes. *Small Rumin. Res.* **2024**, *231*, 107201. [CrossRef]

80. Di Sotto, A.; Mancinelli, R.; Gulli, M.; Eufemi, M.; Mammola, C.L.; Mazzanti, G.; Di Giacomo, S. Chemopreventive Potential of Caryophyllane Sesquiterpenes: An Overview of Preliminary Evidence. *Cancers* **2020**, *12*, 3034. [CrossRef] [PubMed]
81. Ka, H.; Park, H.J.; Jung, H.J.; Choi, J.W.; Cho, K.S.; Ha, J.; Lee, K.T. Cinnamaldehyde induces apoptosis by ROS-mediated mitochondrial permeability transition in human promyelocytic leukemia HL-60 cells. *Cancer Lett.* **2003**, *196*, 143–152. [CrossRef]
82. Bakkali, F.; Averbeck, S.; Averbeck, D.; Idaomar, M. Biological effects of essential oils—A review. *Food Chem. Toxicol.* **2008**, *46*, 446–475. [CrossRef] [PubMed]
83. Zhang, X.; Guo, Y.; Guo, L.; Jiang, H.; Ji, Q. In Vitro Evaluation of Antioxidant and Antimicrobial Activities of Melaleuca alternifolia Essential Oil. *Biomed. Res. Int.* **2018**, *2018*, 2396109. [CrossRef]
84. Wondrak, G.T.; Cabello, C.M.; Villeneuve, N.F.; Zhang, S.; Ley, S.; Li, Y.; Sun, Z.; Zhang, D.D. Cinnamoyl-based Nrf2-activators targeting human skin cell photo-oxidative stress. *Free Radic. Biol. Med.* **2008**, *45*, 385–395. [CrossRef]
85. Anwar, S.; Almatroudi, A.; Allemailem, K.S.; Jacob Joseph, R.; Khan, A.A.; Rahmani, A.H. Protective Effects of Ginger Extract against Glycation and Oxidative Stress-Induced Health Complications: An In Vitro Study. *Processes* **2020**, *8*, 468. [CrossRef]
86. Pazyar, N.; Yaghoobi, R.; Bagherani, N.; Kazerouni, A. A review of applications of tea tree oil in dermatology. *Int. J. Dermatol.* **2013**, *52*, 784–790. [CrossRef] [PubMed]
87. Algefare, A.I.; Alfwuaires, M.; Famurewa, A.C.; Elsawy, H.; Sedky, A. Geraniol prevents CCl(4)-induced hepatotoxicity via suppression of hepatic oxidative stress, pro-inflammation and apoptosis in rats. *Toxicol. Rep.* **2024**, *12*, 128–134. [CrossRef]


**Disclaimer/Publisher's Note:** The statements, opinions and data contained in all publications are solely those of the individual author(s) and contributor(s) and not of MDPI and/or the editor(s). MDPI and/or the editor(s) disclaim responsibility for any injury to people or property resulting from any ideas, methods, instructions or products referred to in the content.